ATTACHMENT 2

Report No: SIR-84-022
Revision 0
SI Project No: TVA-04
July 20, 1984

# ANALYSIS OF BROWNS FERRY UNIT 3 JET PUMP INSTRUMENTATION NOZZLE SAFE-END REPAIR

Prepared by
Structural Integrity Associates, Inc.

Prepared for
Tennessee Valley Authority

Prepared by: R. Stonesifer Date: 7/30/84

Prepared by: A. Y. Kuo Date: 7/30/84

Prepared by: T. L. Gerber Date: 7/30/84

Reviewed by: J. F. Copeland Date: 7/30/84

Approved by: T. L. Gerber Date: 7/30/84
Project Manager

STRUCTURAL INTEGRITY ASSOCIATES

8408150213

# LIST OF FIGURES

## LIST OF TABLES

# 1.0 INTRODUCTION

Cracking suspected to be IGSCC, has been observed in both of the Browns Ferry Unit 3 jet pump instrumentation nozzle safe-ends. The nozzle/safe-end geometry is illustrated in Figures 1.1 and 1.2, and consists of an approximately 5 inch long, tapered, stainless steel safe-end attaching the low alloy steel reactor vessel nozzle to a pair of eccentric reducers. The safe-end and nozzle are nominally 4 inch in diameter. The reducers join the safe-end to a 12 inch nominal diameter blind-flanged pipe through which the instrumentation tubes are routed.

The UT examinations indicate axially oriented cracks located intermittently around the circumference of the safe-end. The worst crack indication is illustrated in Figure 1.3. The crack is essentially through-wall over the thinnest portion of the safe-end and extends about 3.75 inch from the safe-end/reducer weld toward the nozzle weld. Based on a field replication/metallography method, the entire safe-end is believed to be sensitized.

## 1.1 Repair Design Evolution

The initial assessment of the extent of cracking in the safe-ends suggested that cracking was limited to the thin portion of the safe-end. Since applying the overlay to the entire length of the safe-end would presumably make future UT examination more difficult and would require welding near the low alloy nozzle, an overlay design which stopped the overlay at the thick end of the taper was initially considered. When later examination of the UT data resulted in revised and larger crack length estimates (with the largest crack extending well into the thick portion of the safe-end as illustrated in Figure 1.3), the short overlay design was abandoned and a design which extended the overlay over the entire safe-end was adopted.

The thickness of the overlay has been revised two times. The original design thickness of 0.16 inch was based on the understanding that the cracks were limited to the thinnest portion of the safe-end. After the crack lengths were revised upward, the design calculations were repeated using an upper bound crack length equal to the length of the safe-end (5.5 inch). This

significant increase in the assumed length of the crack resulted in a 0.02 inch increase in the design thickness to 0.18 inch. This overlay thickness was to be achieved with three automatic GTAW heat sink layers.

The second revision to the overlay thickness was to increase it to the final design thickness of 0.25 inch. This increase in the thickness required four weld layers. This increase in the design thickness was adopted in response to NRC concerns relative to multiple axial flaws and some new (unreviewed) information from BMI concerning the appropriate flow stress to use when estimating the structural margin for pipes with axial flaws. Increasing the weld overlay thickness was judged to be the most expeditious way to address these concerns.

## 1.2 Final Repair Design

The final design configuration is shown in Figure 1.4. The effective weld overlay thickness is 0.25 inch and it extends from the transition region of the eccentric reducer to the middle of the original nozzle to safe-end weld. As indicated in the Figure 1.4, the repair includes one layer of SMAW over the cracked region followed by one layer of GTAW over the entire safe-end. Both of these layers are applied with no water in the safe-end. Additional overlay was applied to produce a uniform diameter in the region of the reducer/safe-end weld. Four layers of GTAW were applied to produce the 0.25 inch design thickness over the entire length of the safe-end and a portion of the eccentric reducer. These final GTAW layers were applied with water inside the safe-end.

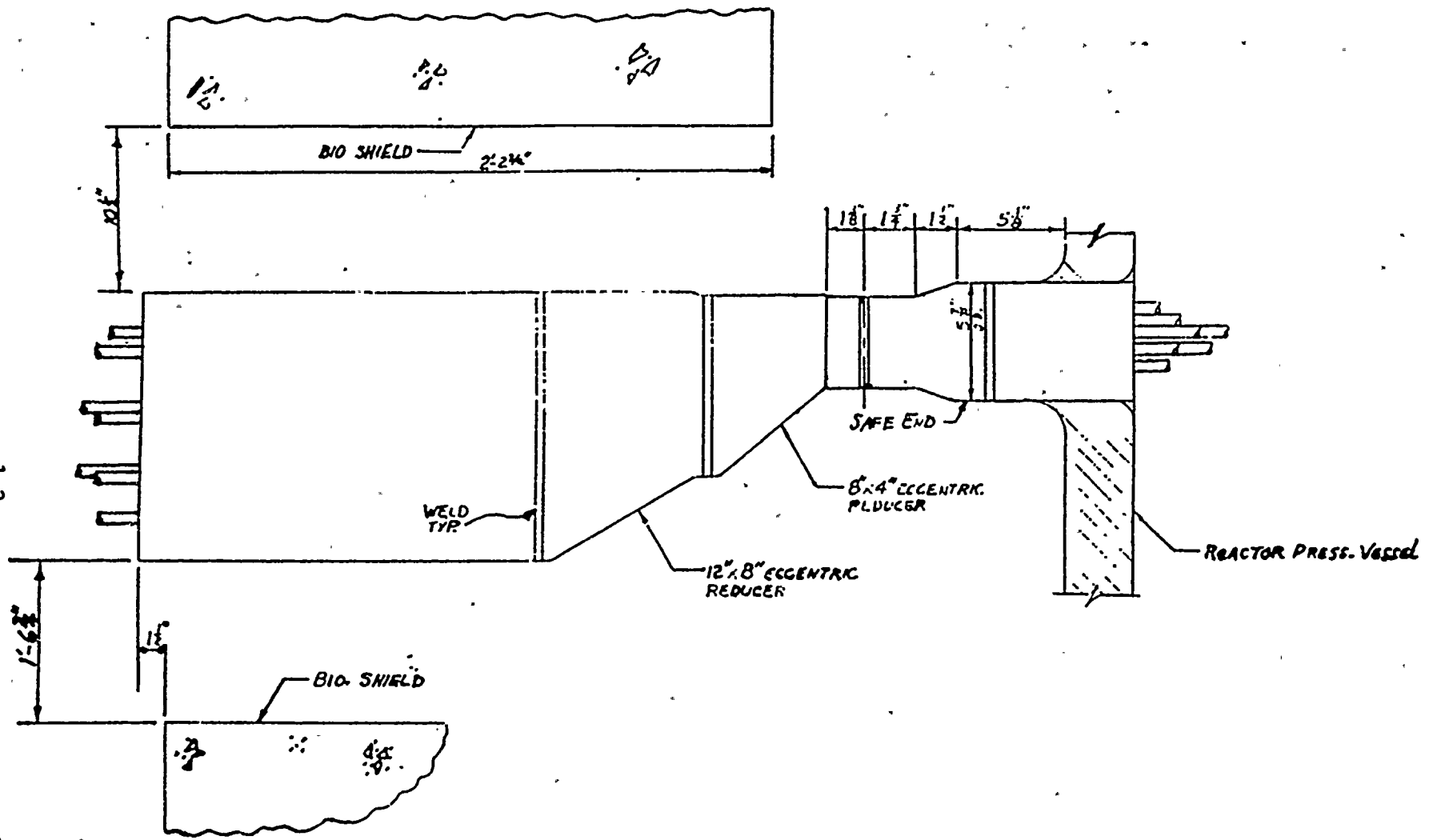


FIGURE 1-1 Jet Pump Instrumentation Nozzle Configuration for Browns Ferry Unit 3 (El. View)

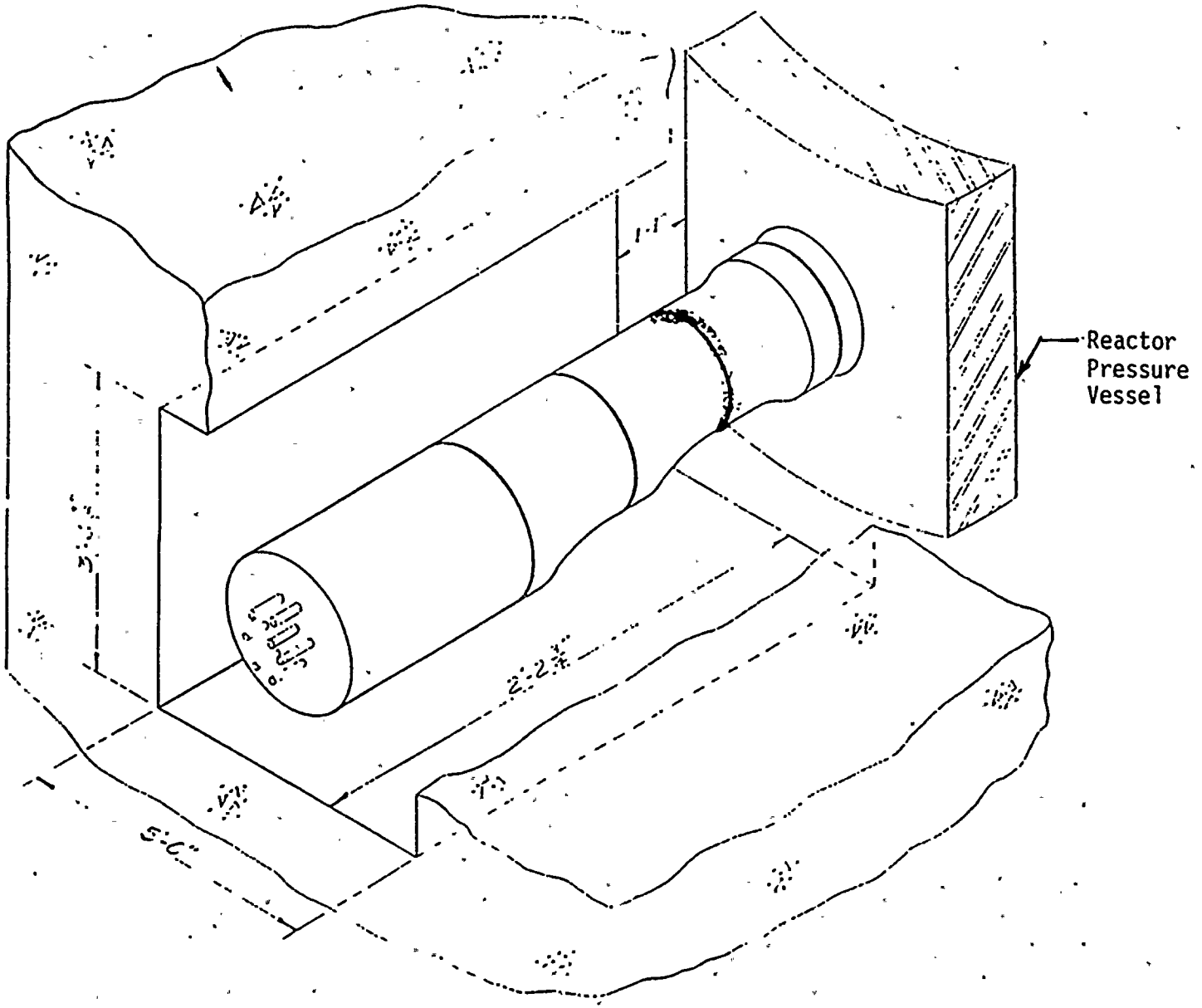


FIGURE 1-2 Jet Pump Instrumentation Nozzle Configuration for Browns Ferry Unit 3 (Perspective)

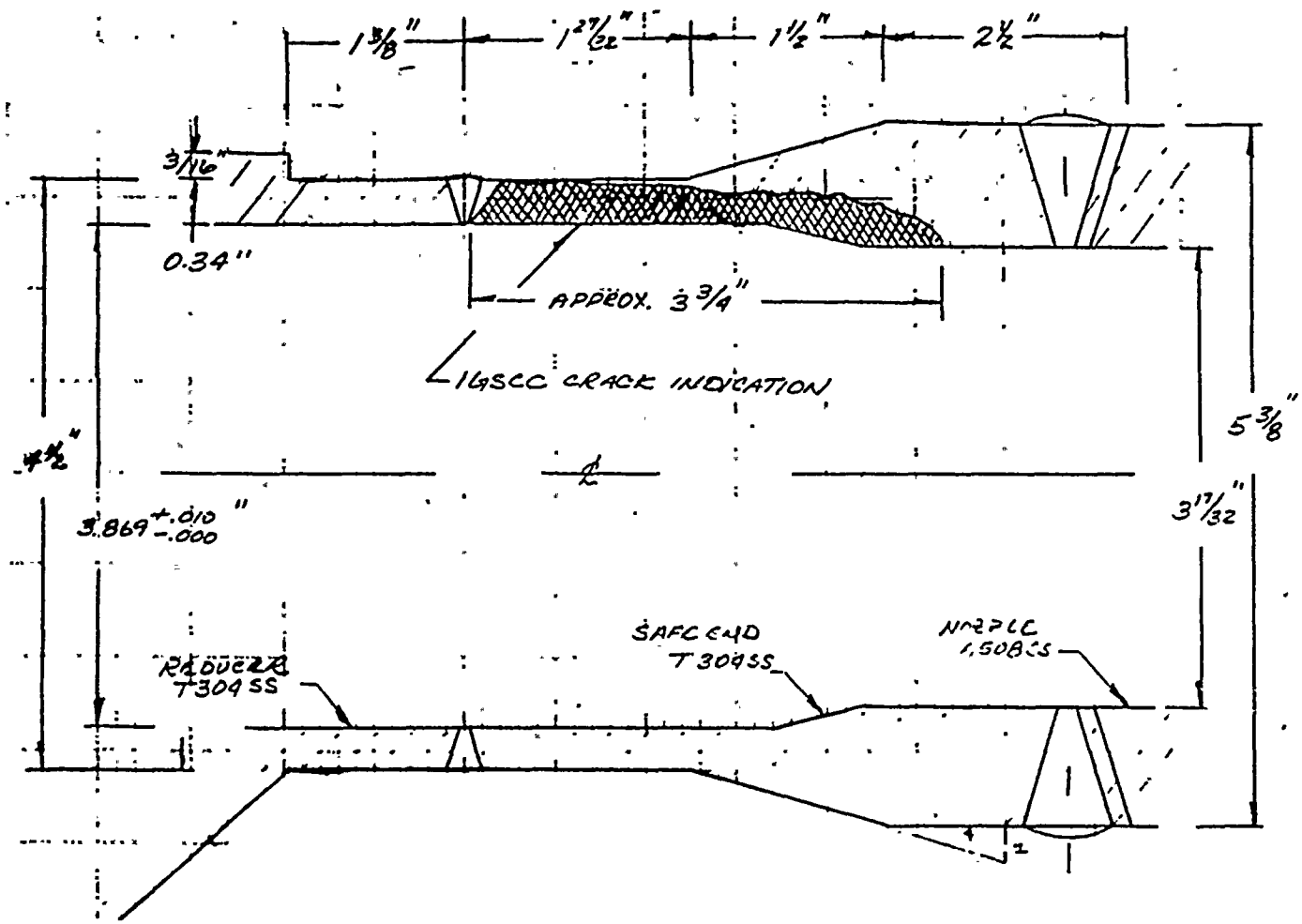


FIGURE 1-3 Cross Section of Safe-End Showing the Worst Observed Crack Indication

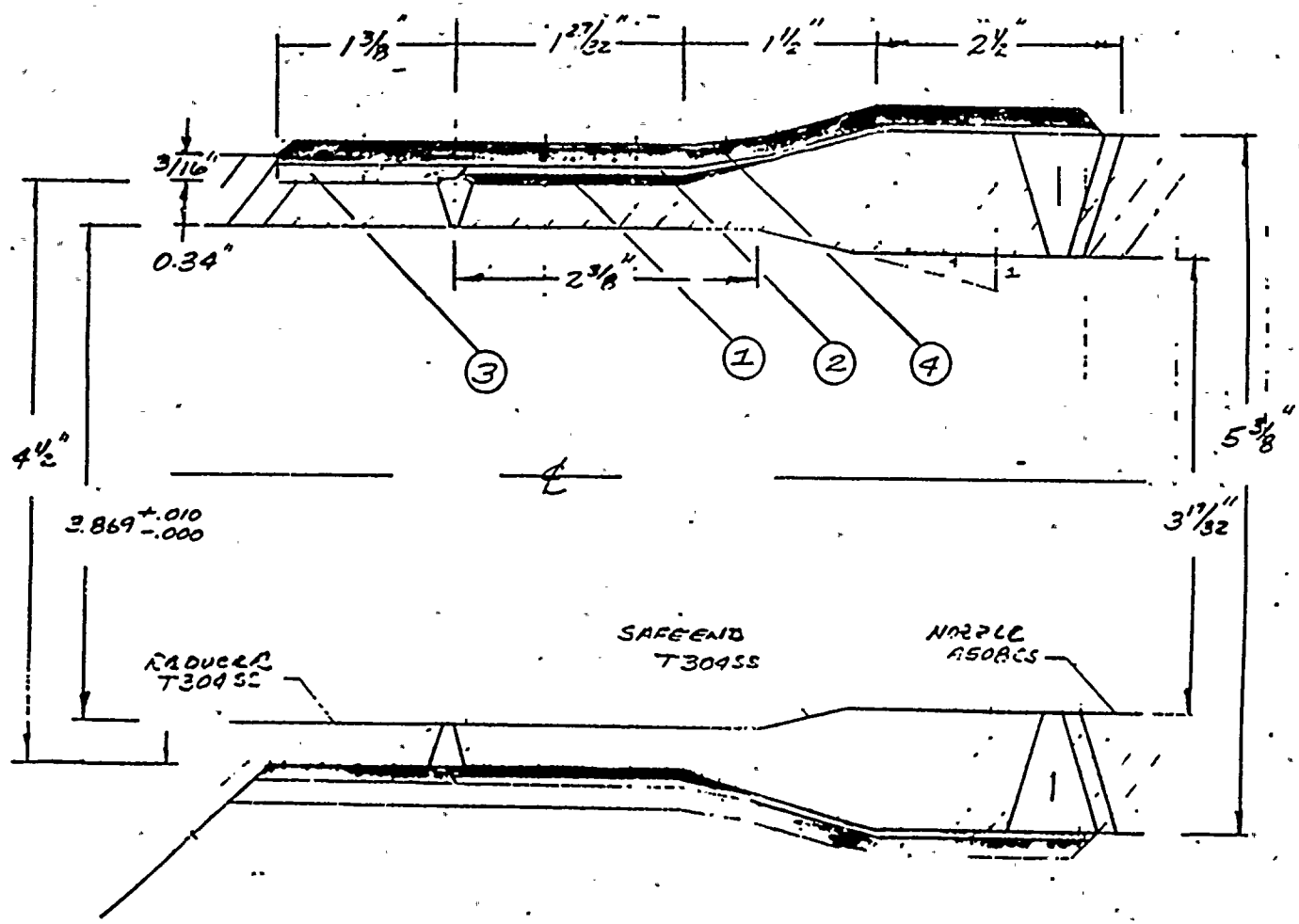


FIGURE 1-4 Final Weld Overlay Design

(1) Stick (SMAW), 1 Pass, Dry Pipe

(2) Auto (GTAW, 1 Pass, Dry Pipe

(3) Auto (GTAW), 2 or 3 Passes, Wet Pip

(4) Auto (GTAW), 4 Passes, Wet Pipe
0.25 Inch Min. Thickness

## 2.0 OVERLAY DESIGN

The weld overlay thickness was sized to meet the requirements of ASME, Section XI, IWB-3640. Both through-thickness, circumferential cracks and through-thickness, full safe-end length (5.5 inch), axial cracks are considered. Using conservative assumptions for safe-end dimensions and loads, an effective overlay thickness of 0.18 inch was found to be adequate. Increasing the overlay thickness from 0.18 to 0.25 inch further increases the structural margin. The design life of the overlay is one fuel cycle, however, it is likely that further analysis, including consideration of subcritical crack growth due to stress corrosion and fatigue, would justify extending the life.

### 2.1 Safe-End Loads and Stresses

Loads for the analysis were obtained from recent design calculations provided by TVA. A design pressure of 1250 psi and axial stresses computed from forces and moments as given in Tables 2.1 and 2.2 (for nozzles N8A and N8B, respectively) were employed to size the repair. Tables 2.3 and 2.4 summarize the calculations of the applied axial stresses at the thinnest section of the safe-end.

### 2.2 Overlay Sizing

The overlay thickness was determined by calculating the thickness required for a worst case axial flaw and for a worst case circumferential flaw and then taking the larger thickness of the two. In the following two subsections, it is shown that the required thickness for the assumed axial flaw is 0.18 inch and the required thickness for the assumed circumferential flaw is 0.16 inches. Therefore, the axial flaw is the one which determines the required overlay thickness of 0.18 inches.

In accordance with NRC SECY-83-267C, the effective overlay thickness is defined as the thickness of overlay deposited after the first weld layer that clears dye penetrant inspection. Also, the minimum effective overlay

thickness permitted was two weld layers after the first layer to clear PT inspection.

2.2.1 Axial Flaws

The methodology of ASME Section XI Table IWB-3641-3 was used to establish the overlay thickness for a 5.5 inch long through-wall axial crack in the safe-end. This was the approximate length of the safe-end.

The stress ratio for use in table IWB-3641-3 was computed from the hoop stress due to pressure:

$$\sigma_H = pR/t = 9{,}881 \text{ psi}$$

where: $\sigma_H$ = hoop stress
p = design pressure, 1250 psi
R = safe-end radius, 5.375/2 inch, to bound largest radius
t = thickness of safe-end, 0.34 inch, to bound thinnest section

For the Code allowable stress Sm = 16,950 psi (ASME Section III), the stress ratio was conservatively computed as:

$$\sigma_H/Sm = 0.583$$

Using an axial crack length ($l_f$) of 5.5 inch and a minimum value of $\sqrt{Rt}$ = 0.825

$$\frac{l_f}{\sqrt{Rt}} = 6.7 \approx 7$$

By employing the above values for the stress ratio and flaw size, Table IWB-3641-3 was used to iterate and reach a solution for the minimum overlay thickness as follows:

(1) Assume the overlay thickness = 0.18 inch

(2) The ratio of crack depth to repaired wall thickness (a/t) was 0.34/(0.34 + 0.18) = 0.654.

(3) The reduced stress ratio due to the overlay thickness was (0.583)x (0.654) = 0.381.

(4) For a stress ratio = 0.381, IWB-3641-3 permits an a/t as large as 0.66. Since the repaired crack depth ratio was 0.654, the overlay thickness of 0.18 inch is sufficient for this assumed axial crack.

2.2.2 Circumferential Flaw

The methodology of ASME Section XI Table IWB-3641-1 was used to determine the required overlay thickness for a bounding 360 degree through-wall crack in the safe-end at the 0.34 inch thickness weld zone.

The axial stress ratio for use in Table IWB-3641-1 were taken from Tables 2.3 and 2.4. The resulting primary stress ratios are:

N8A: (Pm + Pb)/Sm = (4163 + 7998)/16,590 = 0.717

N8B: (Pm + Pb)/Sm = (4186 + 7476)/16,950 = 0.688

where Pm was the primary membrane stress and Pb was the primary bending stress. (Thermal expansion stresses are not included in the stress ratio based on reasoning given in Section 2.4).

Employing these stress ratios and a 360 degree crack size, Table IWB-3641-1 was used to iterate and reach a solution for the minimum overlay thickness as follows:

(1) Assume the overlay thickness to be 0.16 inch

(2) The ratio of the crack depth to repaired wall thickness (a/t) was 0.34/(0.34 + 0.16) = 0.68.

(3) The reduced stress ratio due to the overlay thickness was (0.717)x (0.68) = 0.488.

(4) For a stress ratio of 0.488, IWB-3641-1 permits an a/t of up to 0.687, by extrapolation verified with source equations for net section plastic collapse (Figure 2.1). Since the repaired crack depth ratio was 0.68, the overlay thickness of 0.16 inch was sufficient for the assumed circumferential crack.

This 0.16 inch thickness was smaller than the 0.18 inch thickness required by the assumed axial flaw and thus the required overlay thickness was 0.18 inch.

## 2.3 Structural Margin Calculations

As described above, the weld overlay thickness was initially sized to meet the requirements of IWB-3640. Both through-thickness, 360 degree, circumferential cracks and through-thickness, full safe-end length (5.5 inches), axial cracks were considered. Using conservative assumptions for safe-end dimensions and loads, an effective overlay thickness of 0.18 inch was found to be adequate.

Increasing the overlay thickness from 0.18 to 0.25 in. increases the structural margin. The margin above IWB-3640 requirements can be found by calculating the stress ratio allowed by Code (allowable stress divided by Sm) and comparing this with the applied stress ratio (applied stress divided by Sm) for the repaired safe-end.

Three idealized geometries were considered for the structural margin analysis. In the first, the original safe-end was assumed to be a straight pipe, 0.34 inch thick with a 4.50 inch outside diameter. The second case treats the safe-end as a pipe of 0.92 inch thickness with an outside diameter of 5.38 inches. For these two cases, calculations are made for a through thickness, 5.5 inch long axial crack and a through thickness, 360 degree, circumferential crack.

The third case neglects the original safe-end entirely (or assumes the original safe-end is completely cracked with multiple cracks and thus carries no stress) and looks at the structural margin in the overlay alone. Both hoop and axial stresses were considered.

It should be noted that in the following calculations, no credit was taken for the SMAW and GTAW weld overlay layers applied with the pipe dry (approximately 0.10 inches thickness). These layers increase the thickness of the original safe-end and provide even greater structural margin.

### 2.3.1 Margin for a Through-Wall Axial Flaw

Acceptable stress ratios for piping with axial cracks are provided in ASME Section XI Table IWB-3641-3. This table is based on an empirical formulation attributed to Eiber et al and a safety factor of 3 on the stress to rupture for normal operating conditions (1).

This formulation gives the allowable stress ratio as

$$\frac{\sigma_H}{Sm} = \left[\frac{t/d-1}{t/d-1/M}\right]$$

where M is a curvature correction factor given by

$$M = \left[1+\frac{1.61l^2}{4Rt}\right]^{1/2}$$

and t = wall thickness
R = pipe mean radius
d = crack depth
l = crack length
h = hoop stress
Sm = Code stress limit

If t is the thickness of the original safe-end, let the thickness of the safe-end with the weld overlay repair be t'. In this case, the depth of a through-thickness crack will equal t.

The allowable stress ratio for the repaired safe-end is

$$\frac{\sigma_H}{Sm} = \left[\frac{t'/t-1}{t'/t-1/M}\right]$$

Treating the safe-end as a 4.50 inch diameter pipe with an original wall thickness of 0.34 inch, a through-wall axial crack 5.5 inch long, and a weld overlay repair of 0.25 inch thickness,

allowable $\sigma_H/Sm = 0.51$.

Assuming a design pressure of 1250 psi, the applied stress ratio for this configuration is

applied $\sigma_H/Sm = 0.28$.

The ratio of the allowable stress to the applied stress is then 1.82.

Treating the safe-end as a 5.38 inch diameter pipe with an original wall thickness of 0.92 inch, a through-wall axial crack 5.5 inches long, and a weld overlay repair of 0.25 inch thickness, the Code allowable stress ratio is

allowable $\sigma_H/Sm = 0.35$

while the applied stress ratio for this configuration is

applied $\sigma_H/Sm = 0.17$.

In this case, the ratio of the allowable stress to the applied stress is 2.06.

Review of these factors shows that with either of these idealized safe-end configurations, there is a large margin between the applied stress ratio and the Code allowable stress ratio. Realizing that the Code itself contains a safety factor of 3 on rupture, these margins are significant.

### 2.3.2 Margin for Hoop Stress (neglecting the original safe-end)

Next, consider the case where the original safe-end is neglected or is assumed to have multiple axial cracks. In this case no credit for the original safe-end material is taken and one simply looks at the stress in the 0.25 inch thick overlay. Using the largest overlay radius,

allowable $\sigma_H/Sm = 1.00$

while

applied $\sigma_H/Sm = 0.83$

and the allowable to applied stress ratio is 1.20. Consequently, even if one neglects the original safe-end material, the overlay itself satisfies Code design requirements (which includes a safety factor of 3 on stress to rupture).

### 2.3.3 Margin for a Through-Wall Circumferential Flaw

Acceptable stress ratios for piping with circumferential cracks are provided in ASME Section XI Table IWB-3641-1. Consider first the idealized case in which the safe-end is treated as a 4.5 inch diameter pipe with an original wall thickness of 0.34 inch and a weld repair of 0.25 inch thickness. The original wall is assumed to have a through-wall, 360 degree, circumferential flaw. The repaired flaw depth to thickness ratio is then 0.58. The stress ratios, computed from the stresses of Tables 2.3 and 2.4 and corrected for the repaired wall thickness, are then

N8A: applied (Pm + Pb)/Sm = 0.413

N8B: applied (Pm + Pb)/Sm = 0.396

while the Code allowable stress ratio is

allowable (Pm + Pb)/Sm = 0.70.

Therefore, the ratio of allowable axial stress to the applied axial stress is 1.69 and 1.77 for the N8A and N8B nozzles, respectively.

Next, consider the case in which the safe-end is treated as a 5.38 inch diameter pipe with an original wall thickness of 0.92 inch. Again, assuming a through-wall, 360 degree, circumferential flaw and a weld repair of 0.25 inch thickness, the repaired flaw depth to thickness ratio is 0.79. (The IWB-3640 maximum permitted flaw depth of 0.75 is not of concern here since the actual flaw depth in the thick portion of the safe-end is much less than the assumed through-wall flaw in this discussion.) The applied stress ratios, computed from the stresses of Tables 2.3 and 2.4 and corrected for the repaired wall thickness, are then,

N8A: applied (Pm + Pb)/Sm = 0.214

N8B: applied (Pm + Pb)/Sm = 0.206

while the Code allowable ratio is found by an extrapolation of Figure 2-1

allowable (Pm + Pb)/Sm = 0.28.

Therefore, the ratio of allowable axial stress to the applied axial stress is 1.31 and 1.36 for the N8A and N8B nozzles, respectively.

2.3.4 Margin for Axial Stress (neglecting the original safe-end)

Finally, consider the case where the load bearing capacity of the original safe-end is neglected such that the repaired safe-end is essentially 0.25 inches thick. The axial stress ratios for the 4.5 inch diameter portion of the safe-ends are then

N8A: applied (Pm + Pb)/Sm = 0.851

N8B: applied (Pm + Pb)/Sm = 0.822

while the Code allowable stress ratio is

allowable (Pm + Pb)/Sm = 1.5.

Therefore, the ratio of allowable axial stress to applied axial stress is 1.76 and 1.82 for the N8A and N8B nozzles, respectively.

In fact, even including thermal stresses of 10,556 psi and 9,566 psi for safe end overlays at nozzles N8A and N8B, respectively, the resulting stress ratios are still less than the Code allowable stress ratio of 1.5.

The applied stress ratios for the 5.38 inch diameter portion of the safe-end are smaller than those shown above.

2.4 Weld Metal Toughness Considerations

Experimental and field evidence exists which suggests that some austenitic stainless steel weld metal may be significantly less tough than 304 stainless steel base metal. This raises questions concerning the applicability of the IWB-3640 tables which assume that failure will be due to plastic collapse rather than unstable fracture.

Weld metal toughness is not an issue for the current overlay design because no credit is taken for pre-existing weld metal. That is, the overlay design

is based on assuming through-wall, 360 degree circumferential flaws (as well as long axial flaws). In the current overlay design, the loading can be supported entirely by the high toughness Tungsten Inert Gas (TIG) weld overlay, and thus the IWB-3640 analysis for limit load failure is considered appropriate.

Another issue which is associated with that of toughness is whether secondary stresses, such as thermal stresses, should be included in the IWB-3640 evaluation. If the overlay is sufficiently tough then the failure mechanism will be plastic collapse, the secondary stresses will be, in effect, relieved by the associated large plastic strains. Since the TIG overlay weld is considered to be tough enough that any failure will be by plastic collapse, it would be inconsistent (and overly conservative) to include secondary stresses in the IWB-3640 evaluation.

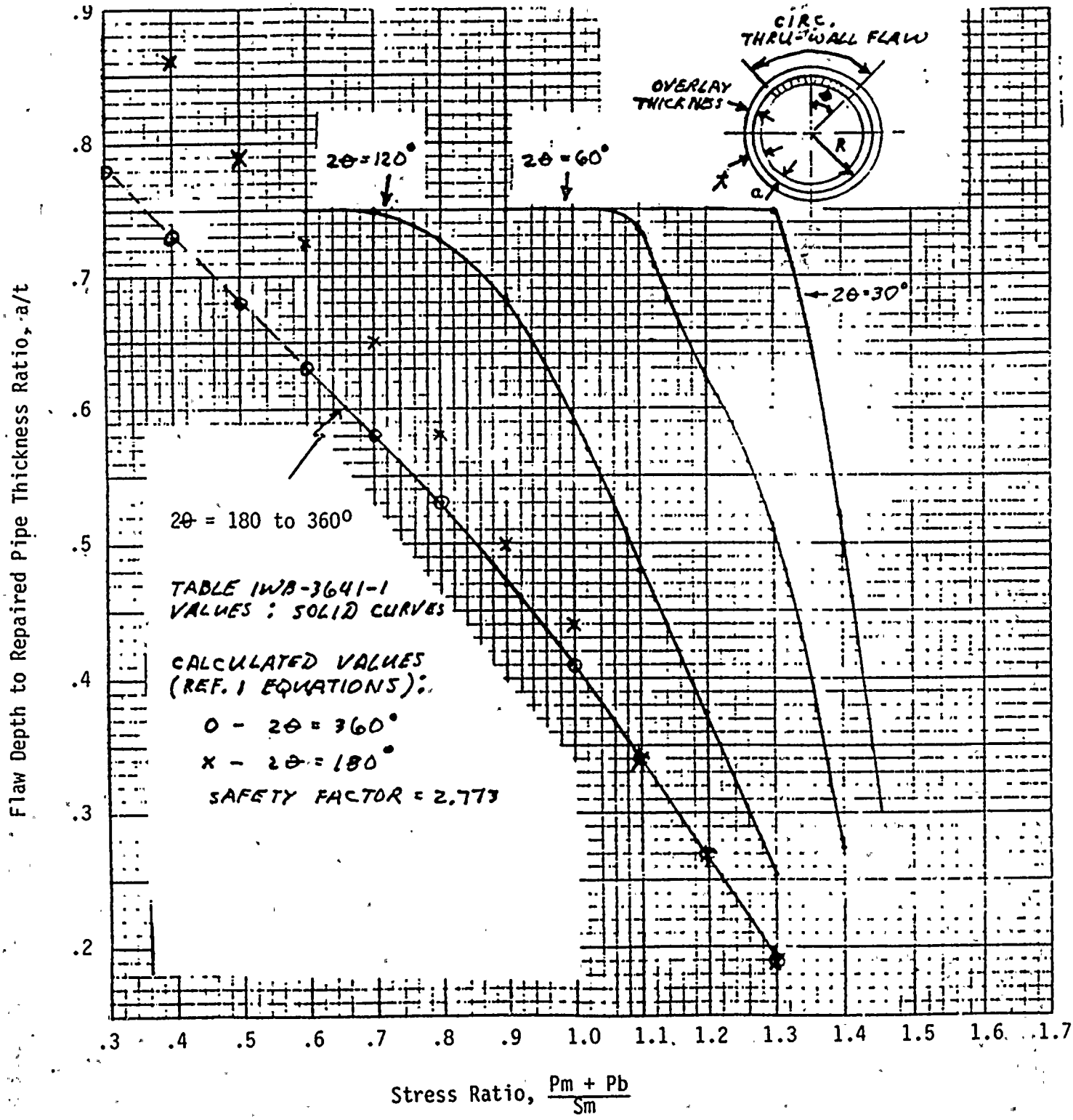


FIGURE 2-1. Circumferential Flaw Size Limits Versus Axial Stress

TABLE 2-1

Applied Loading to Jet Pump
Instrument Nozzle Safe End N8A

| Load | Forces (lbs) | | | Moments (ft-lbs) | | |
|---|---|---|---|---|---|---|
| | $F_x$ | $F_y$ | $F_z$ | $M_x$ | $M_y$ | $M_z$ |
| Deadweight | 33 | -619 | -3 | -18 | 50 | -1682 |
| Thermal | -231 | -1046 | 57 | 132 | -424 | -3666 |
| OBE (±) | 87 | 178 | 268 | 335 | 1042 | 968 |
| SSE (±) | 154 | 297 | 444 | 559 | 1716 | 1595 |

These loads are applied forces and moments from the piping outboard of the safe-end/reducer interface.

TABLE 2-2

Loading to Jet Pump
Instrument Nozzle Safe End N8B

| Load | Forces (lbs) | | | Moments (ft-lbs) | | |
|---|---|---|---|---|---|---|
| | $F_x$ | $F_y$ | $F_z$ | $M_x$ | $M_y$ | $M_z$ |
| Deadweight | 0 | -524 | 0 | 13 | 13 | -1233 |
| Thermal | 52 | -1210 | 0 | 39 | 39 | -3359 |
| OBE (±) | 224 | 360 | 228 | 55 | 880 | 1293 |
| SSE (±) | 241 | 396 | 320 | 72 | 1182 | 1391 |

These loads are applied forces and moments from the piping outboard of the safe-end/reducer interface.

TABLE 2-3

Calculation of Applied Stresses at the
Thinnest Section of Safe-End
at Nozzle N8A

DIMENSIONS

| | |
|---|---|
| OD= | 4.50 IN. |
| ID= | 3.82 IN. |
| T= | .34 IN. |
| A= | 4.44 (IN.) ^2 |
| I= | 9.68 (IN.) ^4 |
| C= | 2.25 IN. |

LOADS (WITHOUT THERMAL STRESS)

| | |
|---|---|
| P= | 1250 PSI |
| FX= | 120 LBS. |
| FY= | 797 LBS. |
| FZ= | 271 LBS. |
| MX= | 353 FT.LBS. |
| MY= | 1092 FT.LBS. |
| MZ= | 2650 FT.LBS. |

AXIAL STRESSES

SM=FX/A + P*R/2*T

= 4163 PSI

SB=MR*C/I

= 7998 PSI

TABLE 2-4

Calculation of Applied Stresses
at the Thinnest Section of Safe-End
at Nozzle N8B

DIMENSIONS

| | |
|---|---|
| OD= | 4.50 IN. |
| ID= | 3.82 IN. |
| T= | .34 IN. |
| A= | 4.44 (IN.)^2 |
| I= | 9.68 (IN.)^4 |
| C= | 2.25 IN. |

LOADS (WITHOUT THERMAL STRESS)

| | |
|---|---|
| P= | 1250 PSI |
| FX= | 224 LBS. |
| FY= | 884 LBS. |
| FZ= | 228 LBS. |
| MX= | 68 FT.LBS. |
| MY= | 893 FT.LBS. |
| MZ= | 2526 FT.LBS. |

AXIAL STRESSES

PM=FX/A + P*R/2*T
= 4186 PSI

PB=MR*C/I
= 7476 PSI

## 3.0 RESIDUAL STRESS ANALYSIS

This section describes the two welding residual stress analyses which were conducted as part of the overlay design process. The analyses provide a means of verifying that the favorable residual stress effects of the overlay procedure do indeed occur for the jet pump instrumentation nozzle safe-end. The unusual aspects of the safe-end which make the residual stress calculations necessary include the proximity of the low alloy steel nozzle and the associated residual stresses from the original nozzle to safe-end weld, the nonuniform thickness of the safe-end, and the presence of a tube sheet which restrains the inward shrinkage of the eccentric reducer during overlay welding.

Two weld overlay lengths were analyzed. In the shorter overlay design, the overlay stops at the thick end of the safe-end outer surface taper, while in the full safe-end length overlay design, the overlay stops on the original safe-end to nozzle weld. Due to the fact that the designs continued to evolve during the time that the overlay residual stress analyses were being made, the analyses do not reflect the final weld overlay designs in all details. However, the results of the calculations clearly show that the beneficial residual stress effects of the heat sink weld overlay process do occur for both overlay lengths.

### 3.1 Background on the Overlay Welding Analysis Methodology

The methodology for numerical modeling of pipe welding techniques was initially developed at Battelle's Columbus Laboratories (2, 3, 4) with support from the Electric Power Research Institute (EPRI) and the U. S. Nuclear Regulatory Commission (NRC). As a result of numerous complexities associated with modeling the welding process and the extreme expense that would be incurred if each aspect of the welding process were modeled with state of the art analytical tools, the methodology uses a number of simplifying assumptions. Most of these assumptions are difficult to justify based solely on analytical reasoning and therefore extensive experimental verification of the methodology has resulted (2-7).

While the weld modeling methodology was developed for pipe girth welds, and the bulk of experimental verification has been for girth welds, the methodology has been applied to other geometries and welding techniques (3, 7). The methodology has recently been applied to the overlay weld repair of a sweepolet and has been found to provide residual stresses which are in good agreement with surface and through-thickness residual stress measurements obtained from a sweepolet mock-up (8).

The methodology for predicting welding residual stress involves the use of two basic models. The first model is used to compute the transient 3D temperature history due to welding. The second model uses this temperature history as input and provides residual stresses, strains, and deflections.

### 3.1.1. Temperature Model

The temperature model is based on the closed form analytical solution for a point heat source moving along a straight path in an infinite medium (2). This solution assumes that thermal properties are independent of temperature and does not include the effect of phase transformations. The principal advantage of using this analytical solution instead of more state of the art numerical solutions is the tremendous cost savings.

Three-dimensional, nonlinear, transient thermal analysis is quite expensive, both computationally and in terms of the time to set up the finite element or finite difference model. The analytical solution on the other hand is amenable to small desktop calculators or microcomputers and requires much less time to exercise.

The most important justification for using this simple model, however, is the fact that it provides a realistic 3D transient temperature history which can be made to fit experimental temperature data through the use of a weld heat input efficiency factor and various other modifications which take advantage of the principle of superposition (e.g., the solution for a doubly insulated plate is easily obtained through superposition methods).

### 3.1.2 Residual Stress Model

The stress analysis model is more sophisticated than the temperature model. The stress model is based on the incremental finite element approach for solving boundary value problems with thermal-elastic-plastic material behavior. Unlike the temperature model, the stress model uses fully temperature dependent mechanical properties.

A primary assumption of the weld modeling methodology is that the welding process can be adequately represented by a two-dimensional stress analysis mode. This assumption is motivated primarily by cost considerations, but through many comparisons with experimental data has been shown to result in good residual stress predictions. The use of axisymmetric models is most common for pipes and similar geometries while plane strain is more appropriate for plates. The residual stress modeling of the safe end is via two-dimensional axisymmetric finite elements.

## 3.2 Short Overlay Welding Analysis

This analysis models the application of three weld overlay layers to the safe-end. The first layer is a 50 kJ/in stick weld which is made without water inside the safe-end. The model assumed that this layer was 0.10 in. thick. The second and third weld layers are automatically deposited 37 kJ/in TIG welds which are each 0.08 inches thick. The safe-end was assumed to be filled with water during these automatic welds. The welding speed was taken as 3 in/min for all weld layers. All three layers extend from approximately 1.0 inch on the eccentric reducer side of the safe-end to reducer weld centerline to about 3.4 inches on the opposite side. This end point coincides with the end of the outer surface taper of the safe-end.

The welding direction was assumed to be circumferential for all welds with the initial weld passes being on the eccentric reducer end of the safe-end and the final weld passes being on the nozzle end. The total thickness of the overlay is 0.26 inches while the thickness of the automatically deposited portion which uses a water heat sink is 0.16 inches.

The finite element grid for the short overlay is shown in Figure 3-1. The two boundries at the upper and left corner of the model are not actual boundaries of the nozzle and are thus provided with "rollers" so as to represent the constraint due the portion of the nozzle which is not modeled. The opposite end of the model is allowed to translate axially but is not allowed to rotate. The safe-end to nozzle weld is represented by a planar transition in material properties from stainless steel to low alloy steel.

The nozzle to safe-end and safe-end to reducer weld induced residual stresses were not simulated in this analysis. In the case of the nozzle weld, this was deemed appropriate due to the separation distance from the overlay. The reducer weld, on the other hand, is directly under the overlay. Experience has shown that final residual stresses are not significantly influenced by the original residual stresses when the butt welded region is totally covered by overlay weld.

The tube support plate inside the reducer was not included in this model. However, it was included in the analysis of the full length overlay. The results of this full length overlay analysis indicate that the tube support plate does not inhibit the residual stress improvement effects of the overlay application for the safe-end, and affects the reducer residual stresses to only a small extent (as will be illustrated in the section pertaining to the full length overlay analysis).

### 3.2.1 Short Overlay Residual Stress Analysis Results

Figures 3-2 and 3-3 show the final hoop residual stress distributions for the short overlay analysis. Figure 3-2 shows the hoop stress isobars for the thin portion of the safe-end and Figure 3-3 shows the hoop stress isobars for the tapered portion of the safe-end. Figures 3-4 and 3-5 show the corresponding plots for the axial stress component. Both stress components are characterized by compressive stress on the inside portion of the section and tensile stress on the outside portion. This type of distribtuion is the intended result of using a heat sink weld.

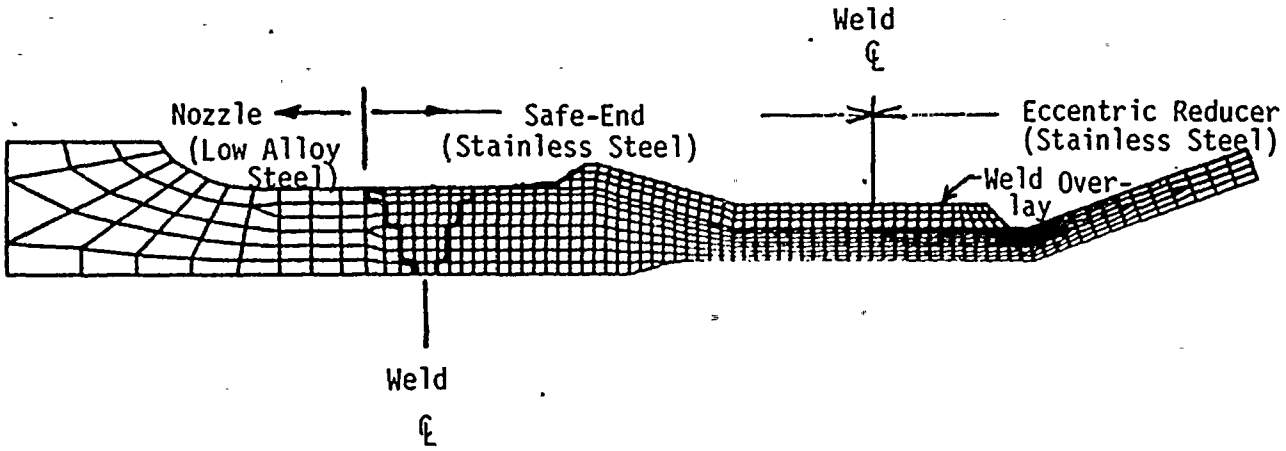


FIGURE 3-1 Finite Element Grid For The Short Overlay Analysis

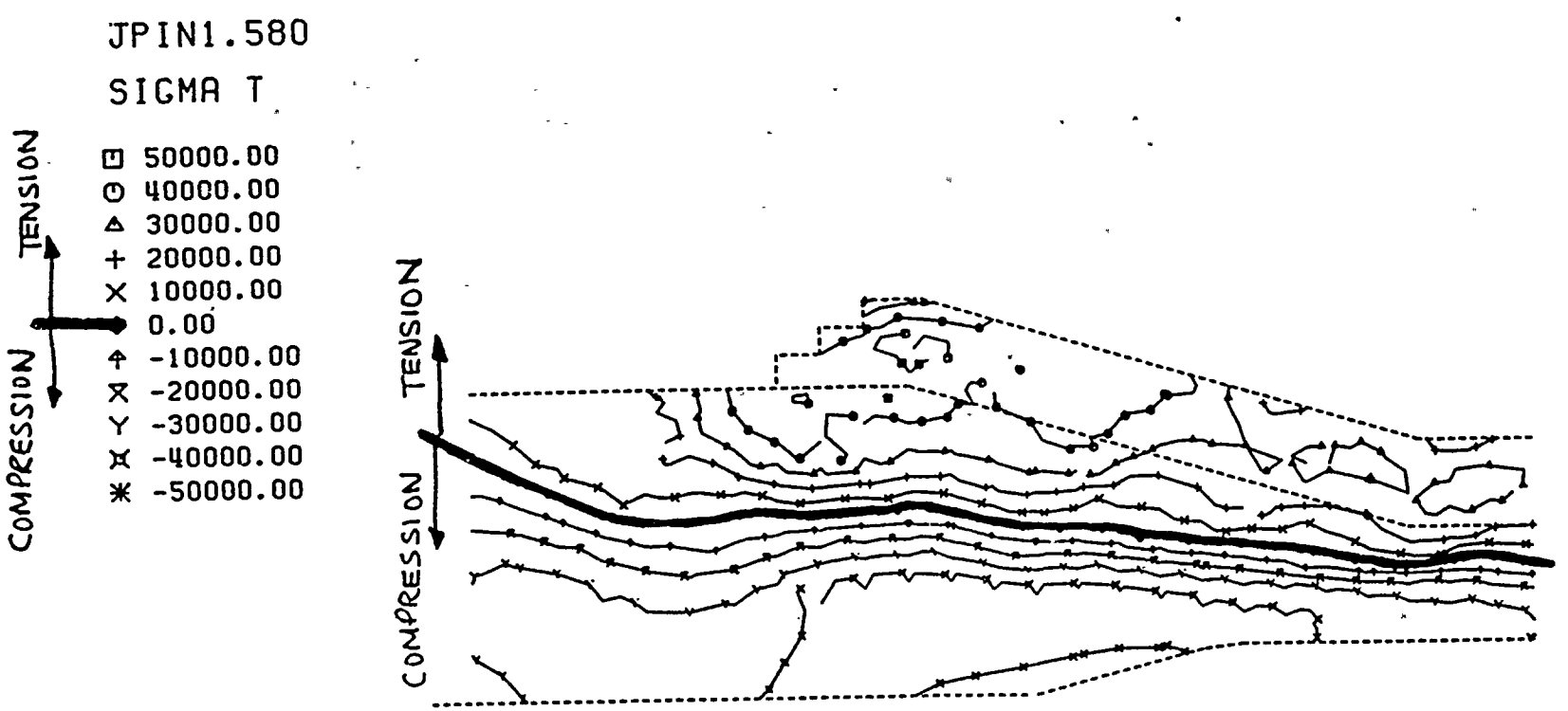


FIGURE 3-2 Residual Hoop Stress Isobars in the Thin Portion of the Safe-End After Completion of the Short Overlay

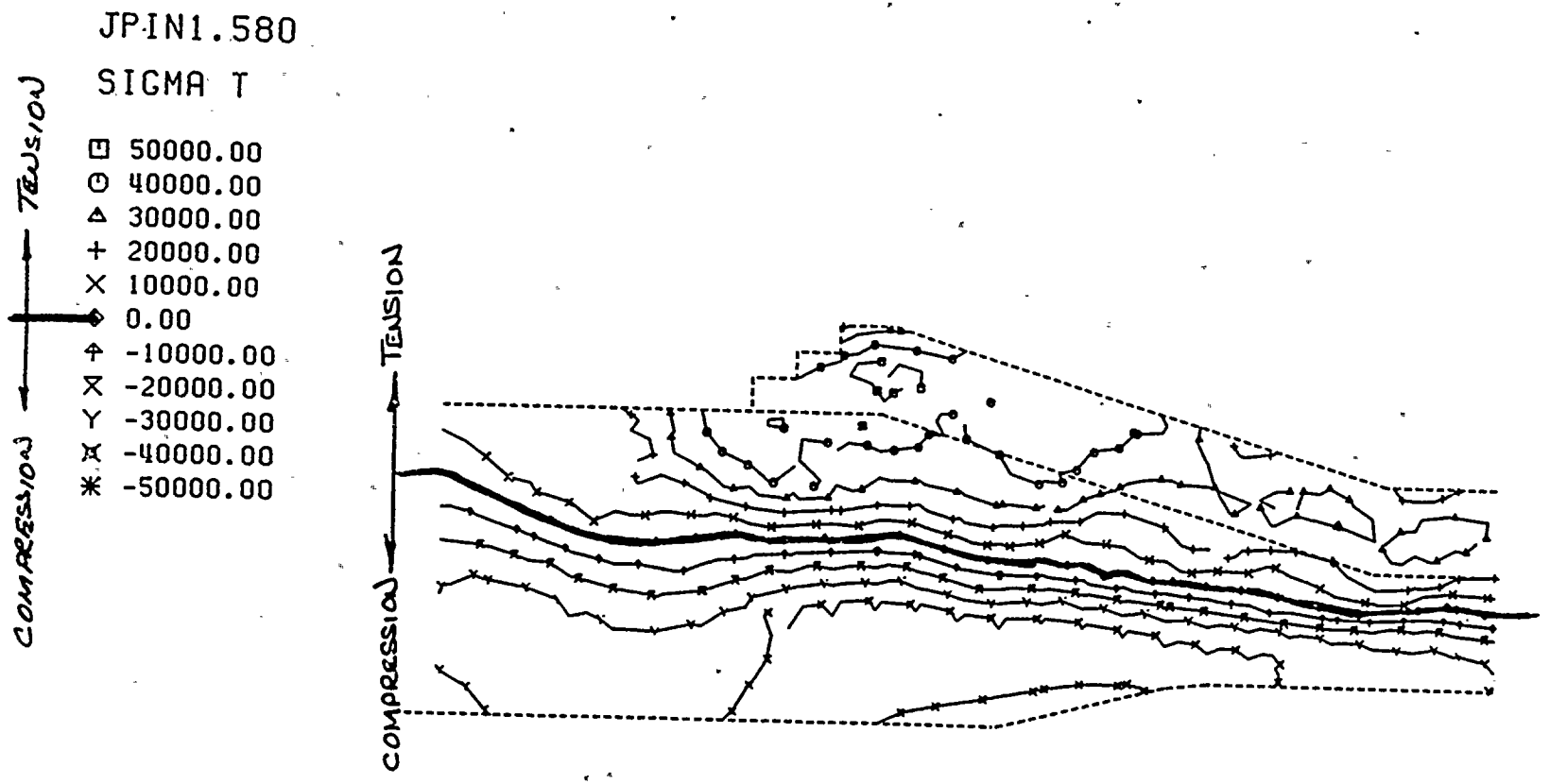


FIGURE 3-3 Residual Hoop Stress Isobars in the Thick Portion of the Safe-End After Completion of the Short Overlay

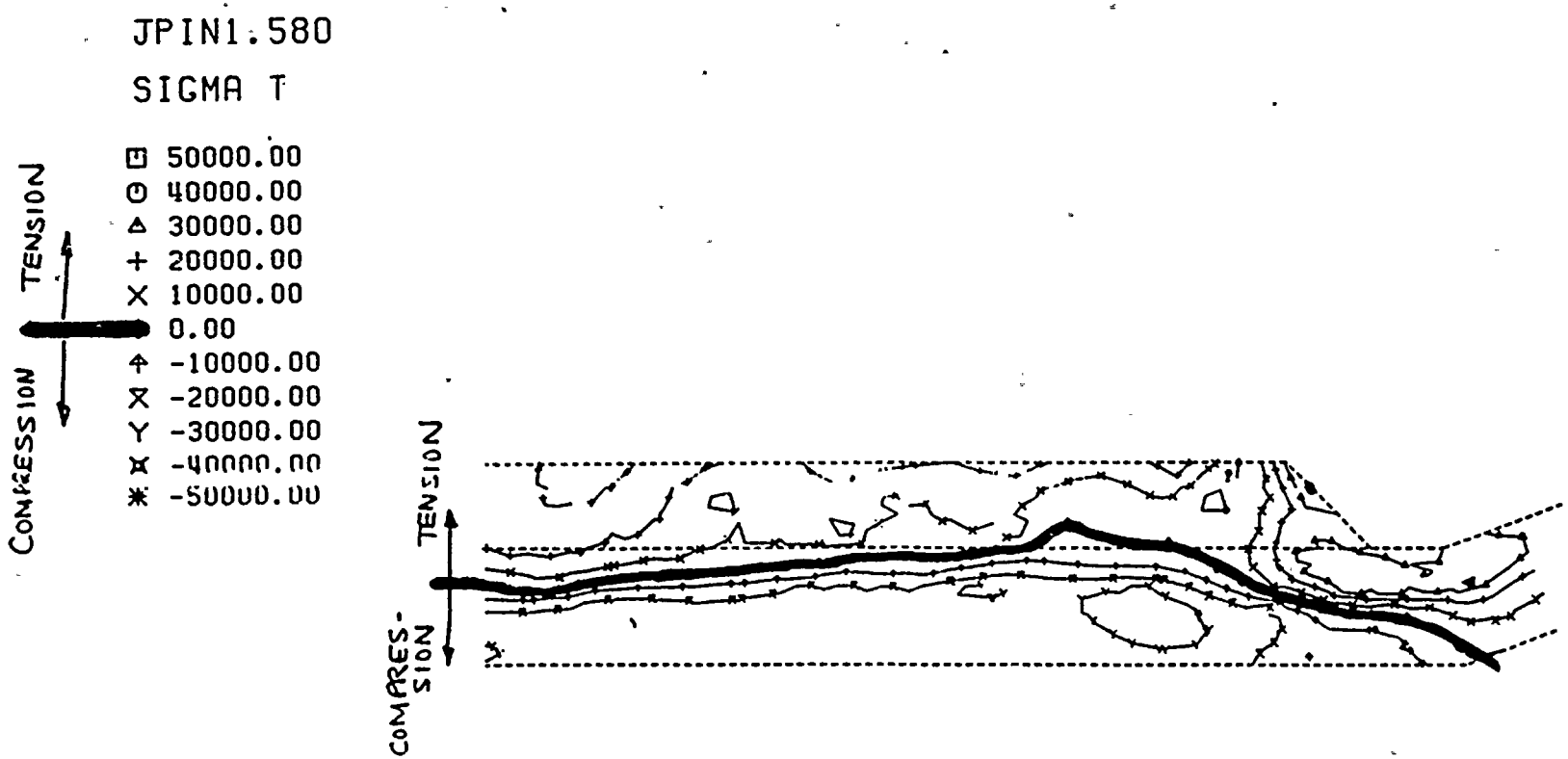


FIGURE 3-4 Residual Axial Stress Isobars in the Thin Portion of the Safe-End After Completion of the Short Overlay

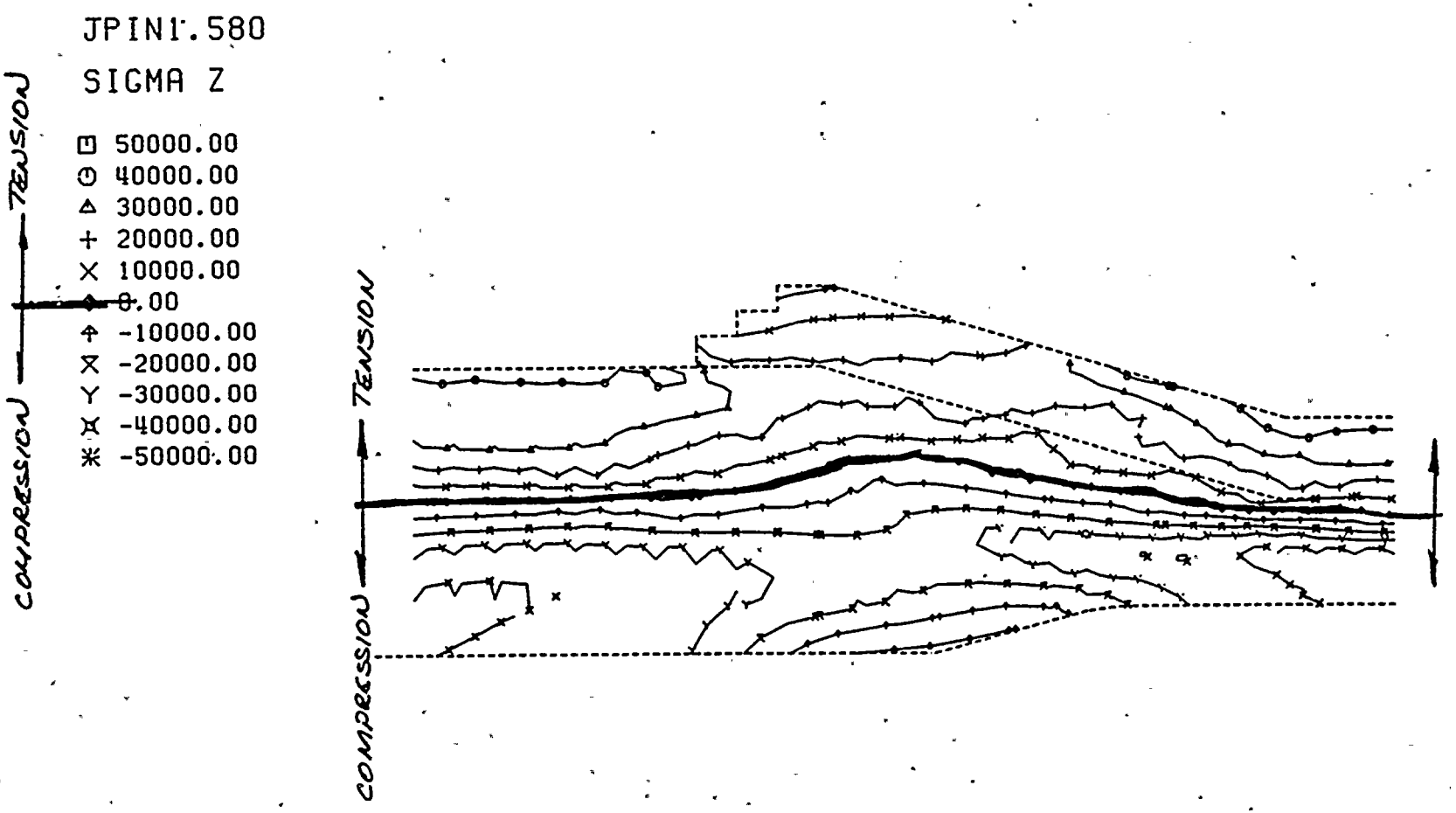


FIGURE 3-5 Residual Axial Stress Isobars in the Thick Portion of the Safe-End After Completion of the Short Overlay

Based on previous experience, the overlay induced residual stresses do not change significantly after the first heat sink layer is deposited. Therefore, depositing one or two additional layers of TIG weld to the overlay would not be expected to significantly alter the residual stresses. Thus the current results are expected to be representative of overlays with as many as four overlay layers.

## 3.3 Full Length Overlay Welding Analysis

This analysis models an overlay which extends from near the transition in the reducer to the middle of the original nozzle to safe-end weld. Due to the original nozzle to safe-end weld being at the edge of the region to be overlaid, any effects of the butt weld residual stresses and/or bimetal interface were included in the analysis by first simulating the nozzle to safe-end butt weld.

Figure 3-6 shows the finite element grid for this full length overlay analysis. The effect of the tube support plate was included in this analysis of the full length overlay. The support plate was modeled as being a rigid support at the inner reducer surface which prevents any inward radial deflection but allows unrestrained outward deflection.

The nozzle to safe-end weld was simulated using ten weld passes applied in six layers. The welding was assumed to be a 50 kJ/in, stainless steel stick weld, being placed at a rate of 3 in/min. While the short overlay analysis approximated the low alloy/stainless steel interface as a radial line, this analysis accurately represents the interface including the weld butter.

After the nozzle to safe-end weld simulation was complete, the application of three weld overlay layers were simulated. The first portion of the first layer is a 50 kJ/in stick weld which is 0.10 in. thick and is made without water inside the safe-end. This stick weld starts at the safe-end to reducer weld and stops at the end of the safe-end outer surface taper. The remainder of the first layer and the second and third layers were modeled as 37 kJ/in GTAW welds with a water heat sink. The second and third

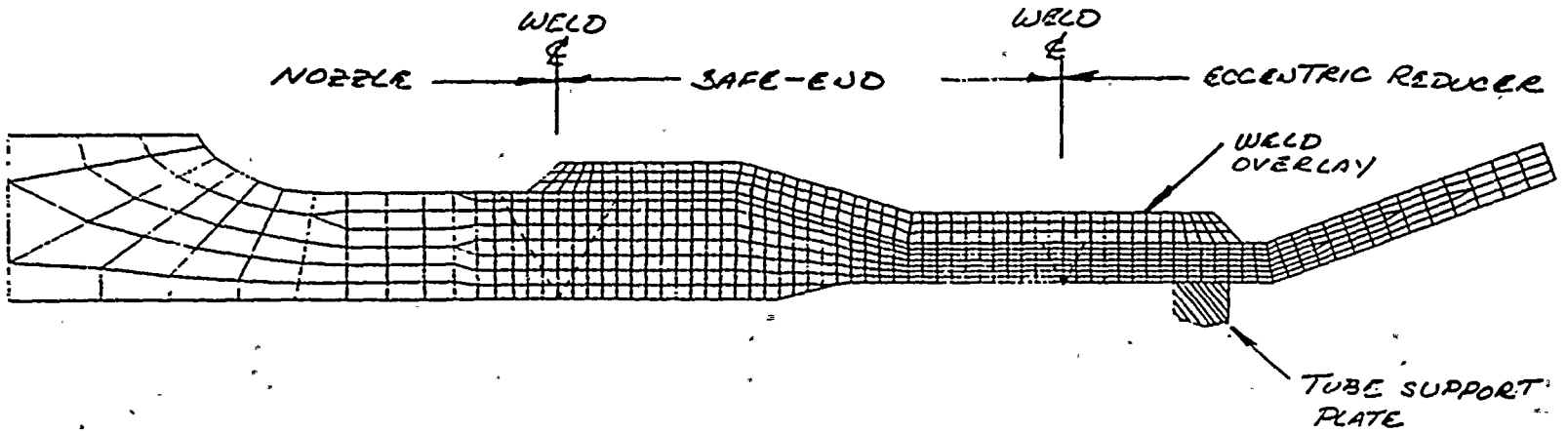


FIGURE 3-6 Finite Element Grid for the Full Length Overlay Analysis

layers are again 0.08 inches thick so that the final overlay thickness, including the non-heat sink layer, is 0.26 inches thick.

The overlay modeled here differs from the final design in two respects. First, in the final design, a non-heat sink weld was applied to the thick portion of the safe-end adjacent to the nozzle while in the model this was applied with a heat sink. This difference does not significantly alter the final residual stresses because the effect of the heat sink is very small at this section due to the large wall thickness. The second difference is the number of overlay layers and the final overlay thickness. As discussed above for the short overlay model, the residual stresses do not change significantly with additional overlay layers and thus the model is believed to provide a good representation of the final overlay design residual stress state.

### 3.3.1 Full Length Overlay Residual Stress Results

Figures 3-7 and 3-8 show the hoop and axial residual stresses in the vicinity of the nozzle to safe-end weld before application of the overlay repair. Note that both stress components are tensile on the inside surface near the weld. The hoop component is highly compressive to either side of the weld and may have been a contributing factor in the tendency for less cracking in the thick portion of the safe-end.

Figures 3-9 and 3-10 show the residual stress in the vicinity of the nozzle to safe-end weld after the overlay repair. In this case, both hoop and axial stresses are compressive over the inner one-half to two-thirds of the original wall thickness. As expected, tensile residual stress is produced in the overlay itself and in the outer portion of the original wall. It is seen that the presence of the nozzle to safe-end weld residual stresses prior to application of the overlay do not adversely affect the overlay induced residual stresses. Furthermore, it would seem that including the nozzle to safe-end weld residual stresses had little effect on the final residual stress state.

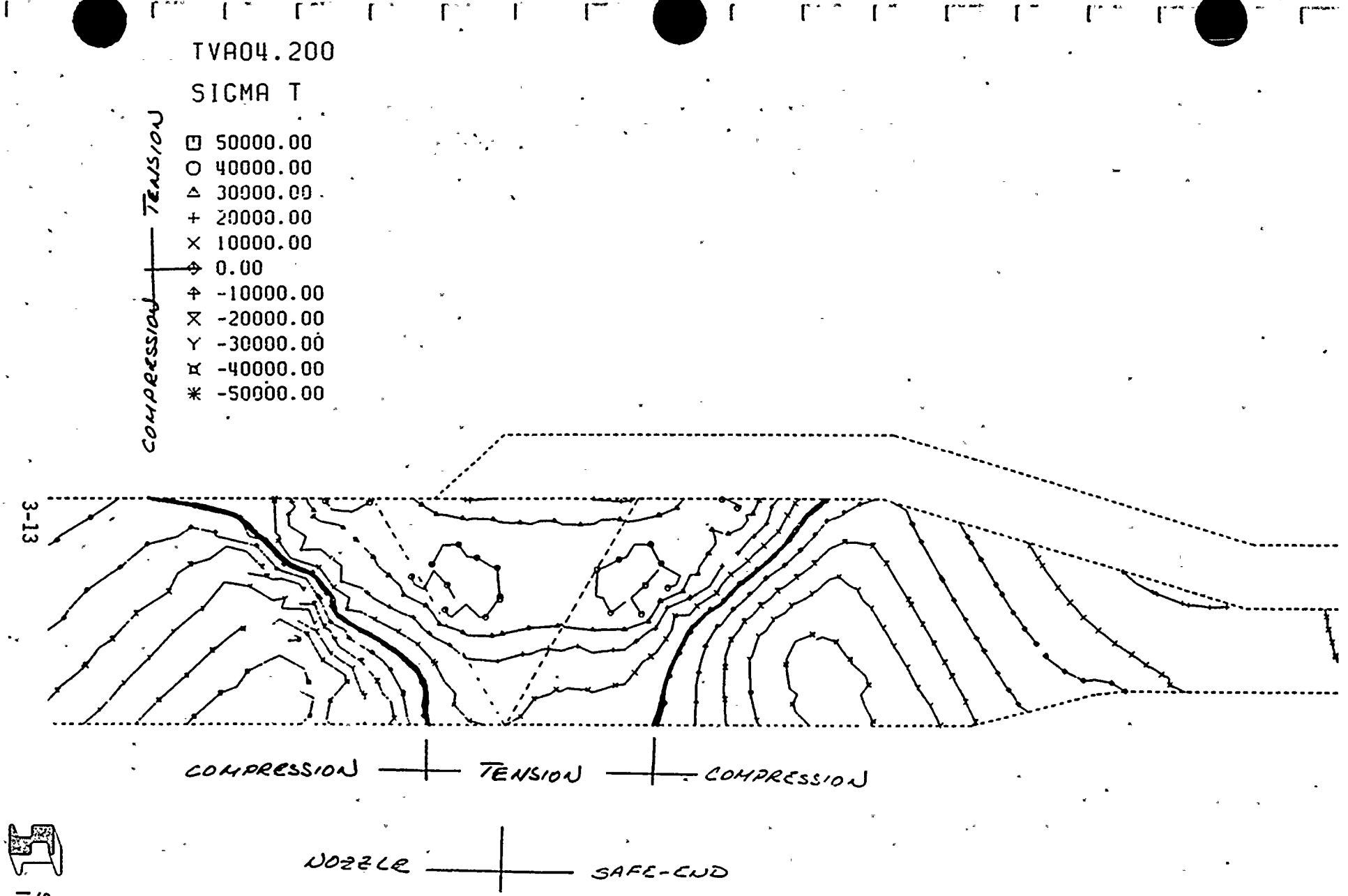


FIGURE 3-7 Nozzle to Safe-End Weld Residual Hoop Stress Before Application of the Overlay

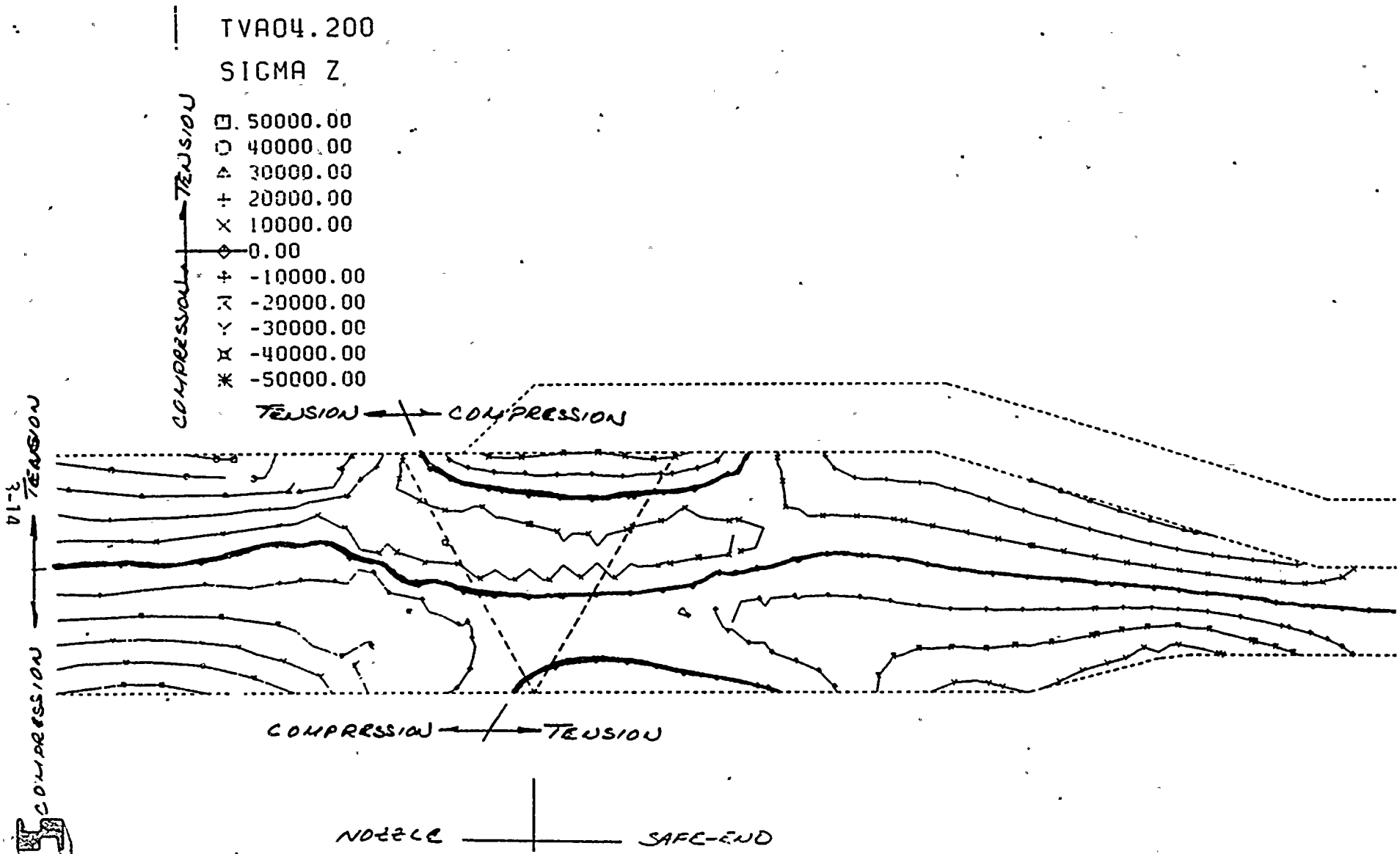


Figure 3-8 Nozzle to Safe-End Weld Residual Axial Stress Before Application of the Overlay

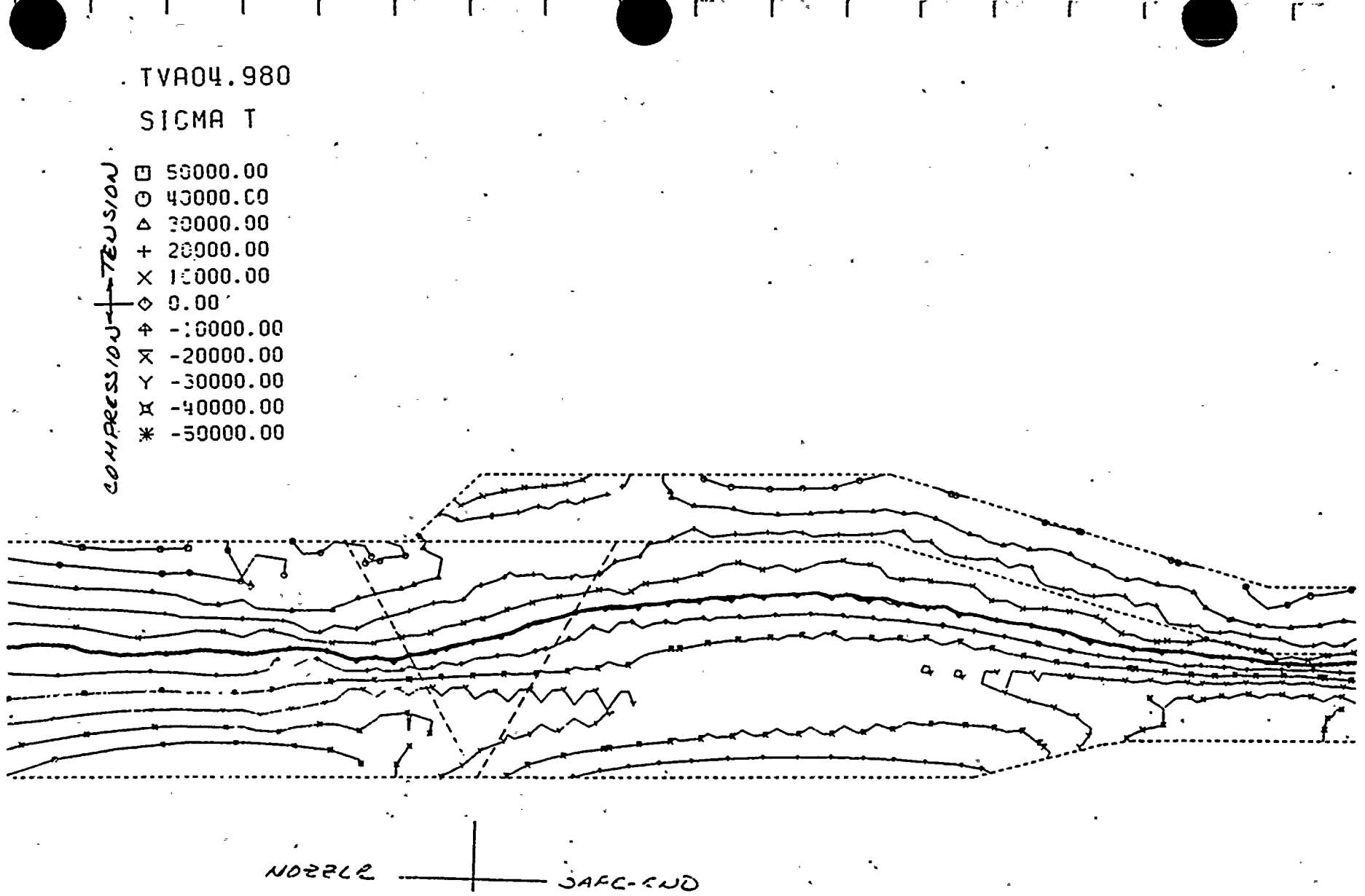


FIGURE 3-9 Nozzle to Safe-End Weld Residual Hoop Stress After Application of the Overlay

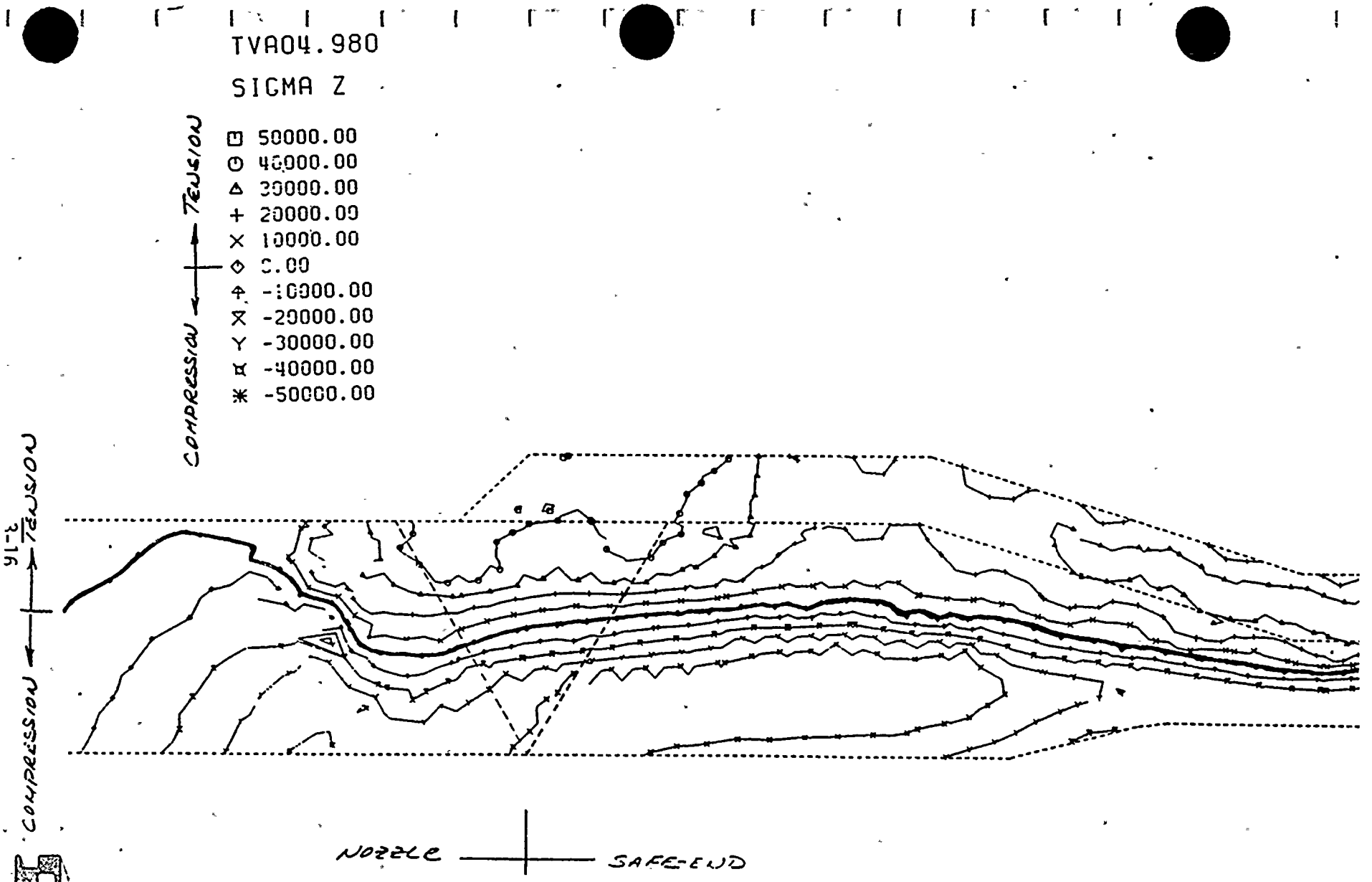


FIGURE 3-10 Nozzle to Safe-End Weld Residual Axial Stress After Application of the Overlay

Figures 3-11 and 3-12 show the predicted residual hoop and axial stress isobars near the safe-end to reducer weld. These results reflect the presence of the tube support plate. These figures can be compared to Figures 3-2 and 3-3 which do not include the effect of the tube support plate. In the reducer, the hoop stresses are less compressive for the case which includes the tube support plate but the hoop stresses in the safe-end are largely unaffected. The axial stresses are largely unaffected by the presence of the tube support plate.

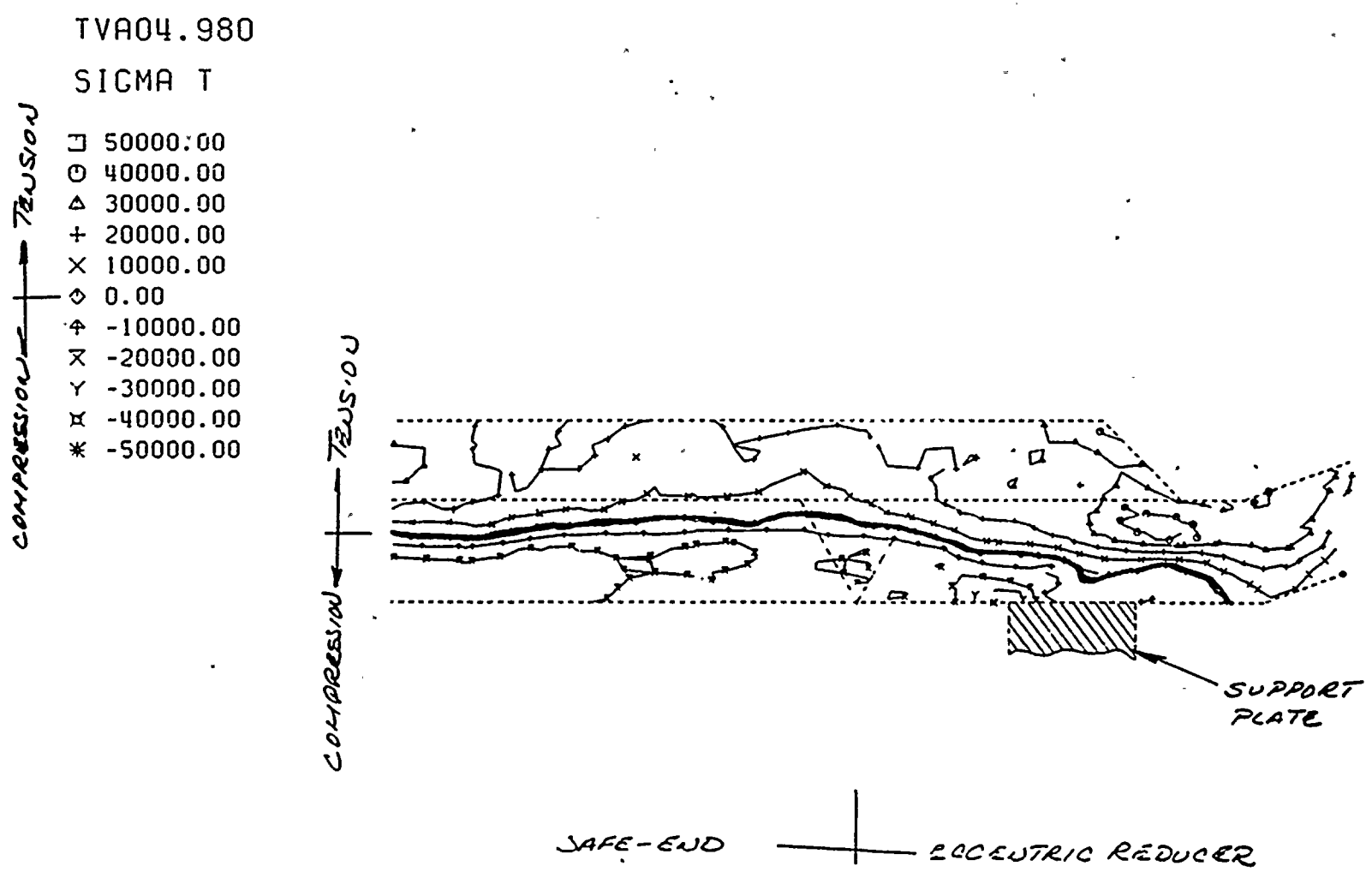


FIGURE 3-11 Residual Hoop Stress Isobars in the Thin Portion of the Safe-End After Completion of the Full Length Overlay (with tube support plate)

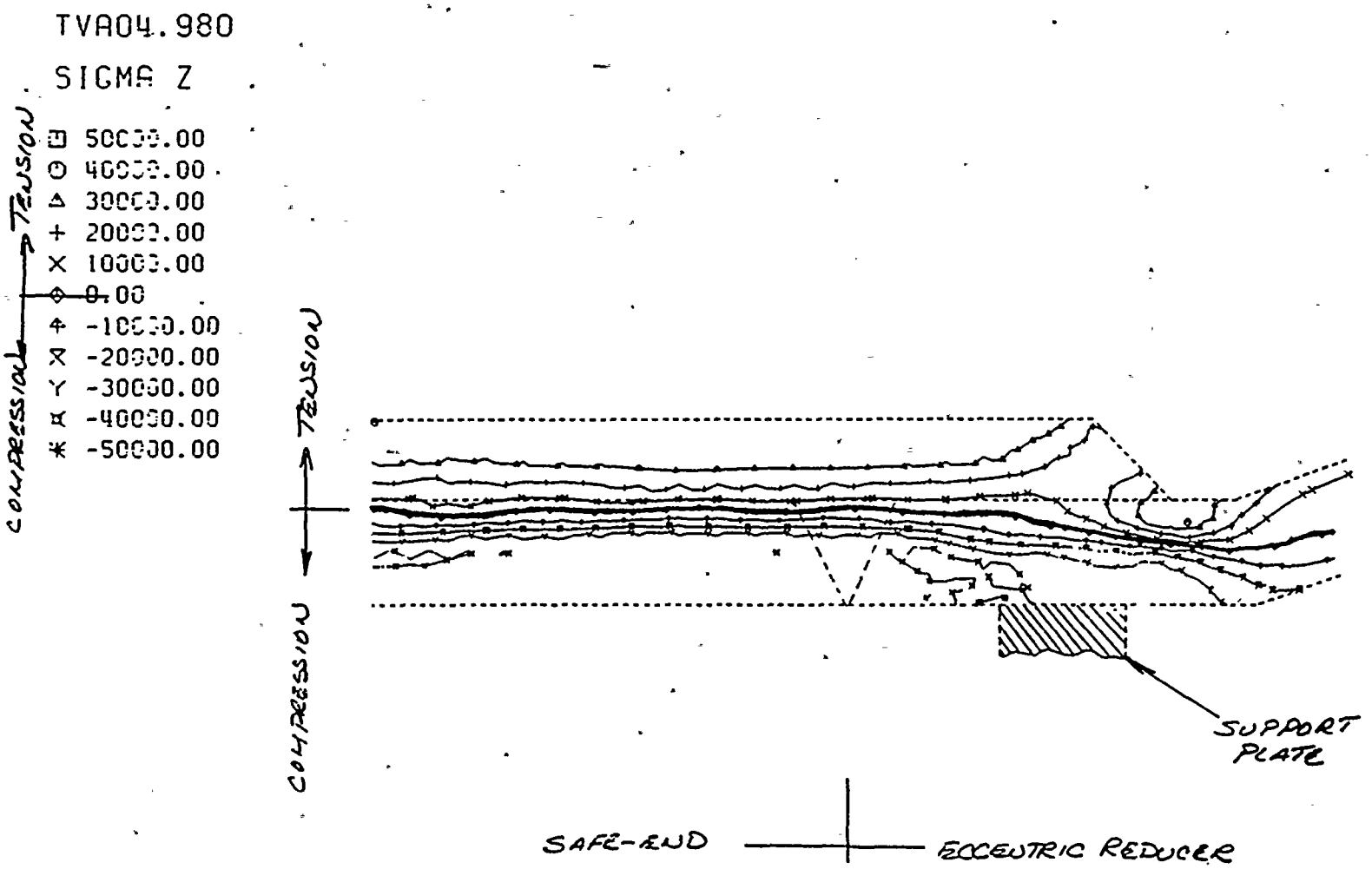


FIGURE 3-12 Residual Axial Stress Isobars in the Thin Portion of the Safe-End after Completion of the Full Length Overlay (with tube support plate)

## 4.0 DISCUSSION AND CONCLUSIONS

Weld overlay repairs have been designed for Browns Ferry Unit 3 jet pump instrumentation nozzle safe-ends in which IGSCC cracks have been identified. The repair configuration consists of multiple layers of weld overlay covering the entire safe-end and applied from the change-in-section region of the eccentric reducer to the center of the safe-end to nozzle weld.

The weld overlay repair was designed based on ASME, Section XI, IWB 3640 criteria. Full safe-end thickness, 360 degree, circumferential cracks and full safe-end thickness, full safe-end length (5.5 inch), axial cracks were assumed in the analyses. Safe-end stresses were calculated from TVA supplied loads and conservative combinations of safe-end dimensions. These analyses showed that an effective weld overlay thickness* of 0.18 inch would be sufficient to maintain Code margins reflected in IWB 3640 criteria.

Following initial weld overlay design, a decision was made to increase the effective overlay thickness from 0.18 inch to 0.25 inch. Calculations were made to show the additional structural margin introduced by increasing the overlay thickness. These calculations show that even if one assumes the original safe-end material is removed and only the weld overlay material remains, Code margins are maintained.

Residual stress calculations were made for a short overlay design (which was not used) and for the final full length overlay design which was employed. These calculations show compressive hoop and axial stresses in the inner one-half to two-thirds of the safe-end and reducer wall over the entire length of the overlay. The presence of the tube support plate in the eccentric reducer near the reducer to safe-end weld does not produce tensile residual stress near the inside surface of the reducer or safe-end.

---

*Thickness of overlay applied after a clean dye penetrant examination of initial overlay layers.

Although the weld overlay repairs are designed for one fuel cycle, it is anticipated that a longer design life could be demonstrated by showing that crack extension by stress corrosion and/or fatigue is not a concern.

## 5.0 REFERENCES


1. Ranganath, S. and Norris, D., "Evaluation Procedure and Acceptance Criteria for Flaws in Austenitic Steel Piping".

2. Rybicki, E. F., et al., "Residual Stresses at Girth-Butt Welds in Pipes and Pressure Vessels", Final Report to U. S. Nuclear Regulatory Commission, Division of Reactor Safety, Research under Contract No. AT (49-24)-0293, NUREG-0376, published November, 1977.

3. Rybicki, E. F., et al., "Residual Stresses Due to Weld Repairs, Cladding and Electron Beam Welds and Effect of Residual Stresses on Fracture Behavior", Final Report to U. S. Nuclear Regulatory Commission, Division of Reactor Safety, Research under Contract No. AT(49-24)-0293, NUREG-0559, published December, 1978.

4. Brust, F. W. and Stonesifer, R. B., "Effect of Weld Parameters on Residual Stresses in BWR Piping Systems", Final Report to Electric Power Research Institute, NP-1743, Research Project 1174-1, March 1981.

5. Rybicki, E. F., et al., "A Finite Element Model for Residual Stresses and Deflections in Girth Butt Welded Pipes", Journal of Pressure Vessel Technology, Vol. 100, No. 3, August 1978, pp. 256-262.

6. Rybicki, E. F. and Stonesifer, R. B., "Computation of Residual Stresses Due to Multipass Welds in Piping Systems", Journal of Pressure Vessel Technology, Vol. 101, No. 2, May 1979, pp. 149-154.

7. Rybicki, E. F. and Stonesifer, R. B., "An Analysis Procedure for Predicting Weld Repair Residual Stresses in Thick-Walled Vessels", Journal of Pressure Vessel Technology, Vol. 102, No. 3, 1980, pp. 323-331.

8. Report "Design Report for Recirculation Piping Sweep-o-lets Repair and Flaw Evaluation, Browns Ferry Nuclear Plant Unit 1", SIA Report SIR-83-006, Rev. 0., 10/21/83.

ATTACHMENT 3

In addition to the aforementioned welds inspected pursuant to the unit 3 shutdown order, the following welds were examined ultrasonically with satisfactory results.

A. N1A and N1B, 28-inch recirculation outlet nozzle-to-safe-end.

B. N2A, N2B, N2C, N2D, N2E, N2F, N2G, N2H, N2J, and N2K. Twelve inch recirculation inlet nozzle-to-safe-end.

C. N-8A and N-8B jet pump instrumentation nozzle-to-safe-end weld

D. N-10 2-inch standby liquid control - core differential pressure nozzle-to-safe-end and safe-end-to-pipe welds

E. N-12 A&B 2-inch instrumentation nozzle-to-safe-end and safe-end-to-pipe welds

F. N-11 A&B and N-16 A&B 2-inch water level nozzle-to-safe-end and safe-end-to-pipe welds.

ATTACHMENT 4

METALLOGRAPHIC EVALUATION OF UNIT 3
REACTOR VESSEL SAFE ENDS
BROWNS FERRY NUCLEAR PLANT

The subject evaluations were performed as a followup after crack indications were found in the jet pump instrumentation nozzle safe ends (N8A, N8B). The jet pump instrumentation nozzle safe ends (N8A, N8B), both unit 3 recirculation outlet nozzle safe ends (N1A, N1B), and 2 of the 10 recirculation inlet nozzle safe ends (N2C, N2H) were examined. Since the 10 recirculation inlet safe ends were fabricated from only two heats of material and the 2 safe ends that were checked were from each of these heats, this sample gives adequate confidence of the condition of all recirculation inlet safe ends. The metallographic determination used is an electrolytic oxalic acid etch to simulate the ASTM A262 practice A sensitization test. This test is a visual determination based on the difference in corrosion behavior in the grain boundary area of the sensitized material versus the nonsensitized material. The grain boundaries will be preferentially attacked in a sensitized material, resulting in a "ditched" appearance. The nonsensitized material will be attacked uniformly across the grain, resulting in a "stepped" appearance.

Figures 1 and 2 give the visual results of the testing on nozzles N8A, N8B, N2C, and N2H taken from field replicas. The recirculation outlet nozzles were visually inspected in the field with a microscope since the replication failed to give adequate results. Figure 1 is the jet pump instrument safe ends. Both of these microstructures would be classified as "ditched," although not all the grain boundary area was attacked. (The Practice "A" guideline is that sensitization is indicated when any grain is completely surrounded by ditched grain boundary.) The inlet nozzles (figure 2) and the outlet nozzles (from visual microscopic examinations) were found to have a "stepped" structure, indicating no sensitization.

The attached table gives the carbon content of all the nozzles examined. The examinations included each of the heats of material involved. The N8A and N8B safe ends had excessively high carbon contents (.08 and .09 percent, respectively) and are made from the same heats of material as the outlet nozzle safe ends. The N8A and N8B safe ends apparently received some post-solution annealed heating, possibly during the local stress relief of the girth welds by Ishikawajima-Harima Heavy Industries (IHI). These safe ends were replaced after the furnace stress relief of the individual shell courses but before the final assembly of the shell

courses. The recirculation inlet and outlet nozzles' maximum temperatures were recorded during the local girth weld stress relief. No information is currently available on the maximum temperature that the jet pump instrumentation nozzles or the standby liquid control (SLC) nozzles attained during local stress reliefs.

Summary and Recommendations

1. The jet pump instrumentation nozzle safe ends appear to have been heated into the sensitization range, probably during a stress relief operation of the vessel at IHI.

2. The metallographic results agree with the ultrasonic testing results on these safe ends. Both the N8A and N8B safe ends appeared sensitized, and both have crack-like indications extending beyond the weld heat-affected zones. The large nozzles did not appear sensitized and have not shown cracking during the inspections current to this report.

3. The SLC safe end has been ultrasonically inspected and is free of defects. We therefore do not expect that this safe end is sensitized.

4. The unit 2 vessel was also assembled at IHI, so the same nozzles may be similarly affected. In addition, the jet pump instrumentation nozzle safe ends have carbon contents of .08 and .09 (information supplied by GE). We therefore recommend that these nozzles be metallographically and ultrasonically examined during the next refueling outage.

The unit 1 safe ends are of lower carbon content and were replaced by B&W (with the exception of the recirculation outlet safe ends which were ID clad) after total stress relief of the reactor pressure vessel. We therefore do not expect that the unit 1 jet pump instrumentation nozzle safe ends are sensitized.

TABLE

Heat Numbers and Carbon Content of Unit 3 Nozzle Safe Ends

| | Nozzle No. | Heat No. | Carbon (%) |
|---|---|---|---|
| Recirculation Outlet | N1A | ES-781-4 | 0.08 |
| | N1B | ES-781-5 | 0.09 |
| Recirculation Inlet | N2A | VL-274-1 | 0.06 |
| | N2B | VL-274-1 | 0.06 |
| | N2C | VL-274-1 | 0.06 |
| | N2D | VL-274-1 | 0.06 |
| | N2E | VL-274-1 | 0.06 |
| | N2F | VL-274-2 | 0.07 |
| | N2G | VL-274-2 | 0.07 |
| | N2H | VL-274-2 | 0.07 |
| | N2J | VL-274-2 | 0.07 |
| | N2K | VL-274-2 | 0.07 |
| Jet Pump Instrumentation | N8A | ES-781-4 | 0.08 |
| | N8B | ES-781-5 | 0.09 |


Figure 1A: Results of the oxalic acid etch on nozzle N8A. All the prepared areas appeared to be under-etched as compared with ASTM A262, Practice A, but are etched enough to make a reasonable determination. Note the difference in etching behavior between these nozzles (Figures 1A and 1B) and the inlet nozzles (Figures 2A and 2B).

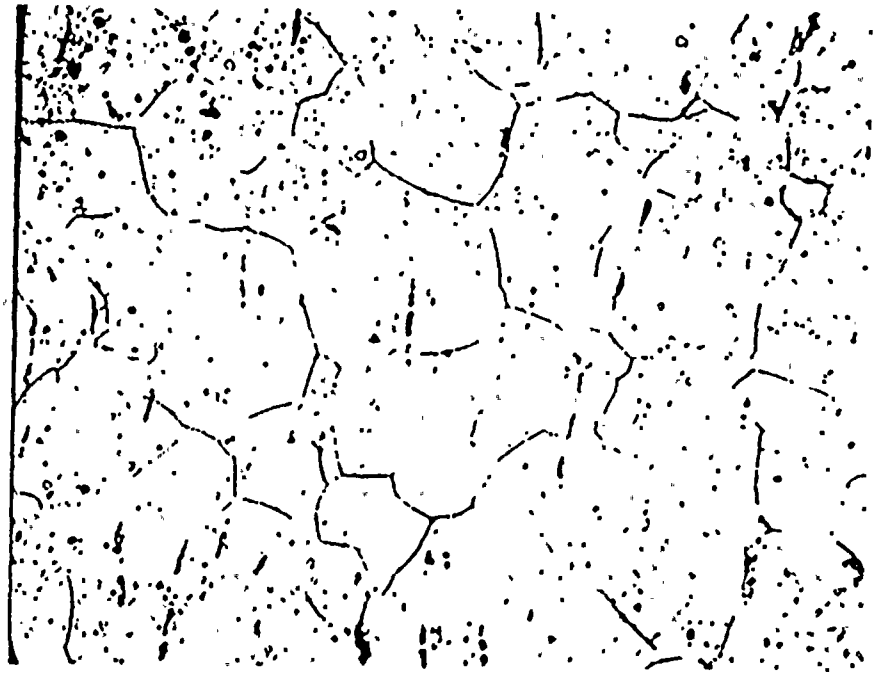


Figure 1B: Nozzle N8B

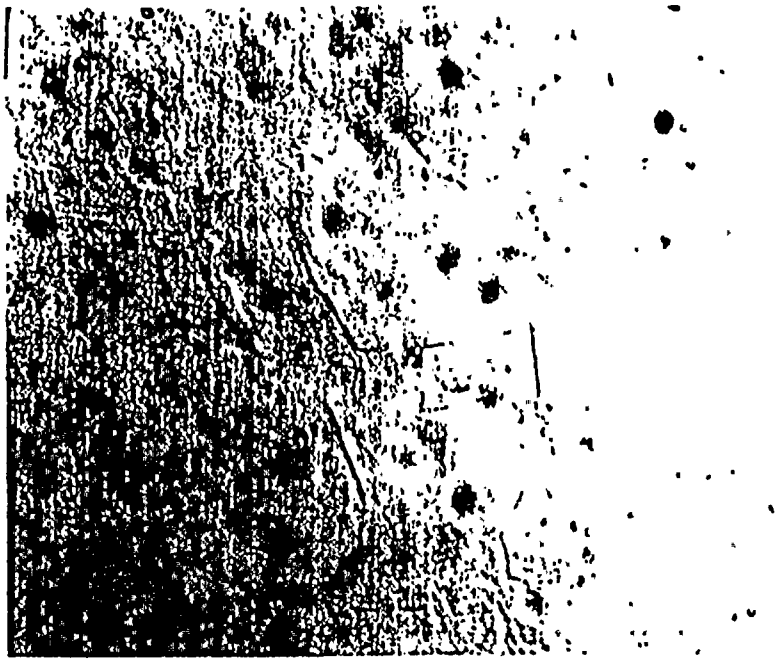


Figure 2A: Nozzle N2C


Figure 2B: Nozzle N2H

ATTACHMENT 5

Browns Ferry Nuclear Plant Unit 3, Cycle 5
Induction Heating Stress Improvement (IHSI)
of IGSCC Susceptible 304 Stainless Steel (SS) Welds

## 1.0 Introduction

Results of the IEB 83-02 IGSCC Ultrasonic (UT) examinations indicated that the recirculation, residual heat removal (RHR), core spray, and reactor water (RWCU) cleanup piping systems were free of indications of IGSCC. To prevent IGSCC initiation, induction heating stress improvement (IHSI) was implemented on all susceptible 304 SS Class 1 welds in those systems.

General Electric Company was contracted to perform IHSI under a two-phase workplan. Phase I consisted of a site survey to evaluate the implementation of IHSI on candidate welds. Phase II included coil development, scheduling, equipment setup, and all other work necessary to complete the IHSI treatments on welds identified as treatable in Phase I.

## 2.0 Phase I - Site Survey

The site survey was conducted from January 22, 1984 through February 3, 1984. The following work was performed during the survey:

- evaluation of candidate welds designated by TVA for treatment
- collection of weld contour data
- verification of weld accessibility and identifica tion of obstructions
- measurement of piping systems - study of potential IHSI equipment locations

The survey information was then evaluated and a workplan for Phase II was laid out.

### 2.1 IHSI Workscope

It was determined that IHSI could be implemented on 147 welds. The treatable welds are listed in Tables 1 through 5 and their locations are shown in figures 1 through 3. Weld DRWC-3-5B, the first outboard isolation valve to flued head weld on the reactor water cleanup system, was added to the scope in May 1984 bringing the total number of treatable welds to 148.

Seven recirculation, 20 core spray, and two RHR welds were excluded from the treatment work scope; these are given in table 6. The recirculation welds which were excluded are fillet welds which could not be treated by then available IHSI methods. IHSI techniques to treat fillet welds are currently under

development, and these welds will be treated at a future outage when such IHSI methods can be used successfully. The core spray and RHR welds which were excluded are carbon steel or low-carbon SS and are not considered susceptible to IGSCC. They will require no further disposition.

## 2.2 Induction Coils

The survey results indicated that 57 induction coils would be needed to perform the 147-weld IHSI work scope. This required 22 new coils in addition to the 35 coils already available to GE.

## 2.3 Interferences

Forty-two interferences were identified during the site survey. The list below gives the type and number of each obstruction identified.

| Type | No. of Obstructions |
|---|---|
| Hanger Lug | 8 |
| Hanger Pad | 3 |
| Hanger Bracket | 6 |
| Hanger Rod | 1 |
| Hanger Clamp | 5 |
| Whip Restraint | 4 |
| Electrical Conduit | 5 |
| Carbon Steel Pipe | 1 |
| Chain Falls and Wire Rope | 4 |
| Snubber Lug | 1 |
| Temporary Scaffold | 2 |
| Clamp | 2 |

The obstructions created by the four whip restraints were avoided by coil redesign. Water-cooled shielding was fabricated to protect the whip restraints from overheating during treatment but was found to be unnecessary as the treatments progressed. All other interferences were removed prior to the treatment of each weld. Plant equipment, such as hanger components and conduit, was restored following treatment of the associated weld.

## 2.4 Equipment

The equipment locations were also determined during the survey. Equipment needed for IHSI consisted of a 4160/480V three-phase transformer, a frequency converter (power supply), work stations, a cooling water system, and a data acquisition system. Each work station consisted of a voltage-reducing transformer, a capacitor bank, and a variable transformer that matches the converter output power to the impedance of the induction coil. The cooling water system was a self-contained closed loop supplying cooling water to the frequency converter, work station, coils and

electrical cables. The data acquisition system monitored and documented the pipe temperature during each IHSI treatment. Thermocouples were attached to the pipe's outer surface and connected to the data acquisition system.

Two work stations were located outside of the drywell, one at each equipment hatchway. The IHSI control room, which housed the data aquisition hardware as well as the process control panel, was located at the personnel air lock. The power supply and cooling supply system pump skid were placed on elevation 593.

In addition, a direct line communication system was established between the power supply, pump skid, heat station, and IHSI control room. A communication line between the IHSI control station and the reactor control room was also established.

## 3.0 Phase II - IHSI Treatments

The IHSI treatments were performed from March 14 through May 25, 1984. The following table shows the time taken to complete each system.

| System | No. Welds | Date First Thermocouple Installed | Date Last Thermocouple Removed |
|---|---|---|---|
| RWCU | 13 | 3/14 | 3/22 |
| CS | 9 | 3/16 | 3/22 |
| Recirc | 96 | 3/23 | 5/14 |
| RHR | 29 | 5/1 | 5/17 |
| Weld DRWC-3-5b | 1 | 5/21 | 5/25 |

An overall average of 3 treatments were performed each day. All treatments were judged to be successful.

In general, the treatment sequence for each weld included thermocouple (TC) installation, coil installation, low-power idle run, coil adjustment, treatment, coil removal, TC removal, and PT of TC tack welds. Selected welds were also ultrasonically examined following the IHSI treatment.

### 3.1 Thermocouples

Eleven TCs were attached to each weld to record temperature data during IHSI treatment. Five TCs were positioned on one azimuth, parallel to the center axis of the pipe, with one centered on the weld crown and two on either side placed in the heat-affected zone (HAZ) and at the edge of the IHSI heat zone. Two TCs were also attached on the HAZ on the three remaining azimuths spaced 90° apart. On some welds, a twelfth TC was used to monitor the temperature of permanent obstructions positioned close to the IHSI heat zone. The data acquisition system had a 12-channel

input, allowing all data to be recorded on tapes, and provided individual TC temperature printouts every 4 seconds. A temperature profile plot was also provided during each IHSI treatment.

The TCs were resistance welded to the pipe in accordance with ASME Section III, NB4311-3. Following the IHSI treatment, the TCs were removed and the affected areas were blended smooth and liquid penetrant examined in accordance with ASME Section III NB5000.

3.2 Low-Power Idle Run

A low-power pre-treatment at 250°C ± 50°C (482°F ± 90°F) was performed on each weld just prior to the full IHSI treatment to verify that the TCs were operative, the coil was positioned correctly, the water was cooling effectively, and load controls were operative. On some welds several low-power tests were required to precisely align the coil.

3.3 IHSI Treatment

To obtain a successful IHSI treatment, the minimum throughwall temperature difference of 275°C (495°F) was effected within the treatment zone for the minimum heating time (see Table 7 for process control parameters). This was achieved by heating the pipe outer surface within the treatment zone to between 400°C (752°F) and 575°C (1067°F) while simultaneously cooling the inner surface with system water flowing at the specified rates. Several welds required more than one attempt to obtain a successful treatment. In the treatment of 31 welds, there were deviations from the process control parameters; these were all determined acceptable by GE engineering and documented on NCR and FDDR reports.

3.4 Post IHSI Ultrasonic Examination

A 25-percent sample of IGSCC susceptible welds were ultrasonically examined following the IHSI treatments. The welds were selected for examination based on the following factors:

1. Welds which had recordable indications and/or underwent evaluation and were found to have geometric reflectors during initial examination for ISGCC.

2. Welds in the same location where defects were found during the unit 1, cycle 5 ISGCC examinations.

The welds in the sample are listed in Table 8. Weld No. DSRWC-3-4 was found to have linear indications. This weld was dispositioned by the Nuclear Central Office Metallurgy and Codes Section as acceptable for continued service. It will be reexamined during the unit 3, cycle 6 inservice inspection.

## 4.0 Conclusions

The IHSI program undertaken on Browns Ferry unit 3 was successfully completed within schedule and without major problems. All IGSCC susceptible 304 SS welds on the subject systems inboard of the penetrations received successful IHSI treatments. The seven recirculation line 4-inch fillet welds, which were not treated, are considered less susceptible to IGSCC than butt welds. As stated previously, these welds are under consideration for future treatment as the technology becomes available.

IHSI has been shown to offer a level of mitigation against IGSCC. Treatment of these recirculation, RHR, core spray, and RWCU will be cost effective by providing one or more cycles of operation with relative freedom from cracking and associated repair activities. Current speculation is that IHSI combined with other mitigation measures, e.g., alternate water chemistry is required to provide life-of-plant immunity.

TABLE.1

RECIRCULATION LOOP A&B

| SIZE (IN.) | CONFIGURATION | LOOP | TVA WELD IDENT. |
|---|---|---|---|
| 28 | STP/SE | A | GR-3-53 |
| " | " | B | GR-3-59 |
| " | STP/LREL | A | KR-3-45 |
| " | " | A | GR-3-54 |
| " | " | A | KR-3-47 |
| " | " | A | KR-3-2 |
| " | " | B | KR-3-50 |
| " | " | B | GR-3-60 |
| " | " | B | KR-3-51 |
| " | " | B | KR-3-24 |
| " | STP/TEE | A | GR-3-55 |
| " | " | A | KR-3-46 |
| " | " | A | KR-3-3 |
| " | " | B | KR-3-25 |
| " | STP/STP | B | GR-3-61 |
| " | VLV/LREL | A | GR-3-56 |
| " | " | A | GR-3-3 |
| " | " | B | GR-3-62 |
| " | " | B | GR-3-29 |
| " | VLV/STP | A | GR-3-57 |
| " | " | A | GR-3-2 |
| " | " | B | GR-3-63 |
| " | " | B | GR-3-28 |
| " | STP/SREL | A | KR-3-48 |
| " | " | B | KR-3-52 |
| " | PMP/SREL | A | GR-3-58 |
| " | " | B | GR-3-64 |
| " | STP/PMP | A | GR-3-1 |
| " | " | B | GR-3-27 |



2/27/84

TABLE 1 (Cont.)

RECIRCULATION LOOP A&B (Cont.)

| SIZE (IN.) | CONFIGURATION | LOOP | TVA — WELD IDENT. |
|---|---|---|---|
| 28 | CRS/TEE | B | GR-3-34 |
| " | CRS/RED | A | KR-3-11 |
| " | " | B | KR-3-33 |
| 22 | HDR/ECP | A | KR-3-15 |
| " | " | B | KR-3-37 |
| " | HDR/CRS | A | KR-3-12 |
| " | " | A | GR-3-18 |
| " | " | B | KR-3-34 |
| " | " | B | GR-3-44 |
| " | HDR/VLV | A | GR-3-25 |
| " | " | A | GR-3-26 |
| " | " | B | GR-3-51 |
| " | " | B | GR-3-52 |
| " | HDR/SOL | A | KR-3-13 |
| " | " | A | KR-3-14 |
| " | " | A | KR-3-19 |
| " | " | A | KR-3-20 |
| " | " | B | KR-3-35 |
| " | " | B | KR-3-36 |
| " | " | B | KR-3-41 |
| " | " | B | KR-3-42 |
| 12 | STP/SOL | A | GR-3-9 |
| " | " | A | GR-3-12 |
| " | " | A | GR-3-19 |
| " | " | A | GR-3-22 |
| " | " | B | GR-3-35 |
| " | " | B | GR-3-38 |
| " | " | B | GR-3-45 |
| " | " | B | GR-3-48 |
| *28 | CRS/TEE | A | GR-3-8 |



* REVISED 3/14/84

TABLE 1 (Cont.)

RECIRCULATION LOOP A&B (Cont.)

| SIZE (IN.) | CONFIGURATION | LOOP | TVA WELD IDENT. |
|---|---|---|---|
| 12 | STP/SE | A | GR-3-11 |
| " | " | A | GR-3-14 |
| " | " | A | GR-3-17 |
| " | " | A | GR-3-21 |
| " | " | A | GR-3-24 |
| " | " | B | GR-3-37 |
| " | " | B | GR-3-40 |
| " | " | B | GR-3-43 |
| " | " | B | GR-3-47 |
| " | " | B | GR-3-50 |
| " | STP/REI | A | GR-3-15 |
| " | " | B | GR-3-41 |
| 5 | WLT/ECP | B | GR-3-63A |
| *4 | " | A | GR-3-4 |
| " | " | A | GR-3-7 |
| " | " | B | GR-3-30 |
| " | " | B | GR-3-33 |
| 12 | STP/LREL | A | GR-3-10 |
| " | " | A | GR-3-13 |
| " | " | A | GR-3-16 |
| " | " | A | GR-3-20 |
| " | " | A | GR-3-23 |
| " | " | B | GR-3-49 |
| " | " | B | GR-3-46 |
| " | " | B | GR-3-42 |
| " | " | B | GR-3-39 |
| " | " | B | GR-3-36 |
| " | " | A | KR-3-16 |



* REVISED 3/19/84

TABLE 1 (Cont.)

RECIRCULATION LOOP A&B (Cont.)

| SIZE (IN.) | CONFIGURATION | LOOP | TVA WELD IDENT. |
|---|---|---|---|
| 12 | STP/LREL | A | KR-3-17 |
| " | " | A | KR-3-18 |
| " | " | A | KR-3-21 |
| " | " | A | KR-3-22 |
| " | " | B | KR-3-44 |
| " | " | B | KR-3-43 |
| " | " | B | KR-3-40 |
| " | " | B | KR-3-39 |
| " | " | B | KR-3-38 |

TABLE 2

RHR LOOP A (SUCTION)

| SIZE (IN.) | CONFIGURATION | TVA WELD IDENT. |
|---|---|---|
| 20 | STP/TEE | DRHR-3-19 |
| " | STP/LREL | DSRHR-3-9 |
| " | STP/LREL | DSRHR-3-10 |
| " | STP/LREL | DSRHR-3-11 |
| " | LREL/VLV | DRHR-3-21 |
| " | STP/VLV | DRHR-3-22 |
| " | STP/VLV | DRHR-3-23 |
| " | STP/SOL (6") | DSRHR-3-8 |

TABLE 3

RHR LOOP B (DISCHARGE)

| SIZE (IN.) | CONFIGURATION | TVA WELD IDENT. |
|---|---|---|
| 24 | TEE/STP | DRHR-3-18 |
| " | STP/VLV | DRHR-3-17 |
| " | VLV/SREL | DRHR-3-16 |
| " | SREL/STP | DSRHR-3-7 |
| " | STP/STP | DSRHR-3-6 |
| " | STP/VLV | DRHR-3-15 |
| " | SREL/VLV | DRHR-3-14 |
| " | SREL/STP/SREL | DSRHR-3-5A<br>DSRHR-3-5 |
| " | STP/SREL | DRHR-3-13 |

RHR LOOP A (DISCHARGE)

| | | |
|---|---|---|
| 24 | STP/TEE | DRHR-3-9 |
| " | STP/VLV | DRHR-3-8 |
| " | SREL/VLV | DRHR-3-7 |
| " | SREL/LREL | DSRHR-3-4A |
| " | STP/LREL | DSRHR-3-4 |
| " | STP/STP | DSRHR-3-3 |
| " | STP/VLV | DRHR-3-6 |
| " | VLV/LREL | DRHR-3-5 |
| " | STP/LREL | DSRHR-3-2 |
| " | STP/SREL | DSRHR-3-1 |
| " | STP/SREL | DRHR-3-4 |

TABLE 4

CORE SPRAY

| SIZE (IN.) | CONFIGURATION | TVA WELD IDENT. |
|---|---|---|
| 12 | STP/STP | DCS-3-13 |
| " | STP/LREL | DSCS-3-7 |
| " | LREL/LREL | DSCS-3-8 |
| " | STP/LREL | DSCS-3-9 |
| " | STP/VLV | DCS-3-14 |
| " | STP/STP | DCS-3-4 |
| " | STP/LREL | DSCS-3-1 |
| " | STP/LREL | DSCS-3-2 |
| " | STP/VLV | DCS-3-5 |

TABLE 5

REACTOR WATER CLEAN-UP

| SIZE (IN.) | CONFIGURATION | TVA WELD IDENT. |
|---|---|---|
| 6 | SOL/VLV | DRWC-3-1A |
| " | VLV/STP | DRWC-3-1 |
| " | STP/LREL | DSRWC-3-1 |
| " | LREL/VLV | DRWC-3-2 |
| " | VLV/STP | DRWC-3-3 |
| " | STP/LREL | DSRWC-3-1A |
| " | LREL/STP | DSRWC-3-2 |
| " | STP/LREL | DSRWC-3-3 |
| " | STP/LREL | DSRWC-3-4 |
| " | STP/LREL | DSRWC-3-5 |
| " | LREL/STP | DSRWC-3-6 |
| " | STP/LREL | DSRWC-3-7 |
| " | STP/LREL | DRWC-3-4 |

TABLE 6

Welds Not Treated By IHSI Process

Recirculation Loop A

KR-3-49
KR-3-4
KR-3-1

Recirculation Loop B

KR-3-26
KR-3-23
KR-3-53
GR-3-63b

Core Spray System

TCS-3-426
TSCS-3-425X
TSCS-3-423
TSCS-3-424
TCS-3-422
TCS-3-421
TSCS-3-420
TCS-3-419
TSCS-3-418
TCS-3-417
TCS-3-410
TSCS-3-409
TSCS-3-408
TSCS-3-407
TCS-3-406
TCS-3-405
TSCS-3-404
TCS-3-403
TSCS-3-402
TCS-3-401

RHR System.

TRHR-3-191
TRHR-3-192

TABLE 7

IHSI PROCESS CONTROL PARAMETERS

| | | |
|---|---|---|
| 1. | Pipe Outer Surface Temperature Within Treatment Zone | 500 + 75°C (932 + 135°F) - 100°C - 180°F |
| 2. | Minimum Throughwall Temperature Difference ( $\Delta T$) | 275°C (495°F) |
| 3. | Maximum Temperature of Weld Crown | 600°C (1112°F) |
| 4. | Minimum Width of Zone Heated to $\Delta T$ | $1.5\sqrt{Rt}$ |
| 5. | Minimum Distance from Weld Center to Boundary of T Minimum | 15 mm (0.6 in) or t/2 (whichever is larger) |
| 6. | Minimum Heating Time | 0.7 $t^{2/}$ seconds |
| 7. | Frequency | 3 to 4 kHz |
| 8. | Induction Coil Length | $3\sqrt{Rt}$ Minimum |
| 9. | Minimum Water Velocity (in vertical or horizontal flooded pipe) | 0.5 m/s (1.64 ft/s) |
| 10. | Minimum Water Velocity (in pipe with air pockets) | 1.2 m/s (4 ft/s) |

R= radius t= wall thickness $\alpha$ =thermal diffusivity

TABLE 8

WELD SAMPLE FOR EXAMINATION AFTER IHSI

## Recirculation

| | |
|---|---|
| GR-3-1 (28") | GR-3-44 (22") |
| GR-3-2 (28") | KR-3-15 (22") |
| GR-3-54 (28") | KR-3-34 (22") |
| GR-3-55 (28") | KR-3-37 (22") |
| GR-3-57 (28") | GR-3-13 (12") |
| GR-3-60 (28") | GR-3-16 (12") |
| GR-3-62 (28") | GR-3-20 (12") |
| KR-3-63 (28") | GR-3-36 (12") |
| KR-3-3 (28") | GR-3-39 (12") |
| KR-3-25 (28") | GR-3-42 (12") |
| KR-3-45 (28") | KR-3-39 (12") |
| KR-3-46 (28") | GR-3-14 (12") |
| KR-3-47 (28") | |
| KR-3-50 (28") | |

## Residual Heat Removal

| | |
|---|---|
| DRHR-3-8 (24") | DSRHR-3-2 (24") |
| DRHR-3-13 (24") | DSRHR-3-4A (24") |
| DRHR-3-14 (24") | DSRHR-3-5 (24") |
| DRHR-3-15 (24") | DSRHR-3-5A (24") |
| DRHR-3-21 (24") | DSRHR-3-10 (24") |
| DRHR-3-19 (20") | |

## Core Spray

| | |
|---|---|
| DCS-3-4 (12") | |
| DCS-3-14 (12") | TCS-3-417 (10") |
| DCS-3-1 (12") | TCS-3-422 (12") |

## Reactor Water Cleanup

| | |
|---|---|
| DRWC-3-1A (6") | PT, best effort UT |
| DSRWC-3-3 (6") | |
| DSRWC-3-4 (6") | |

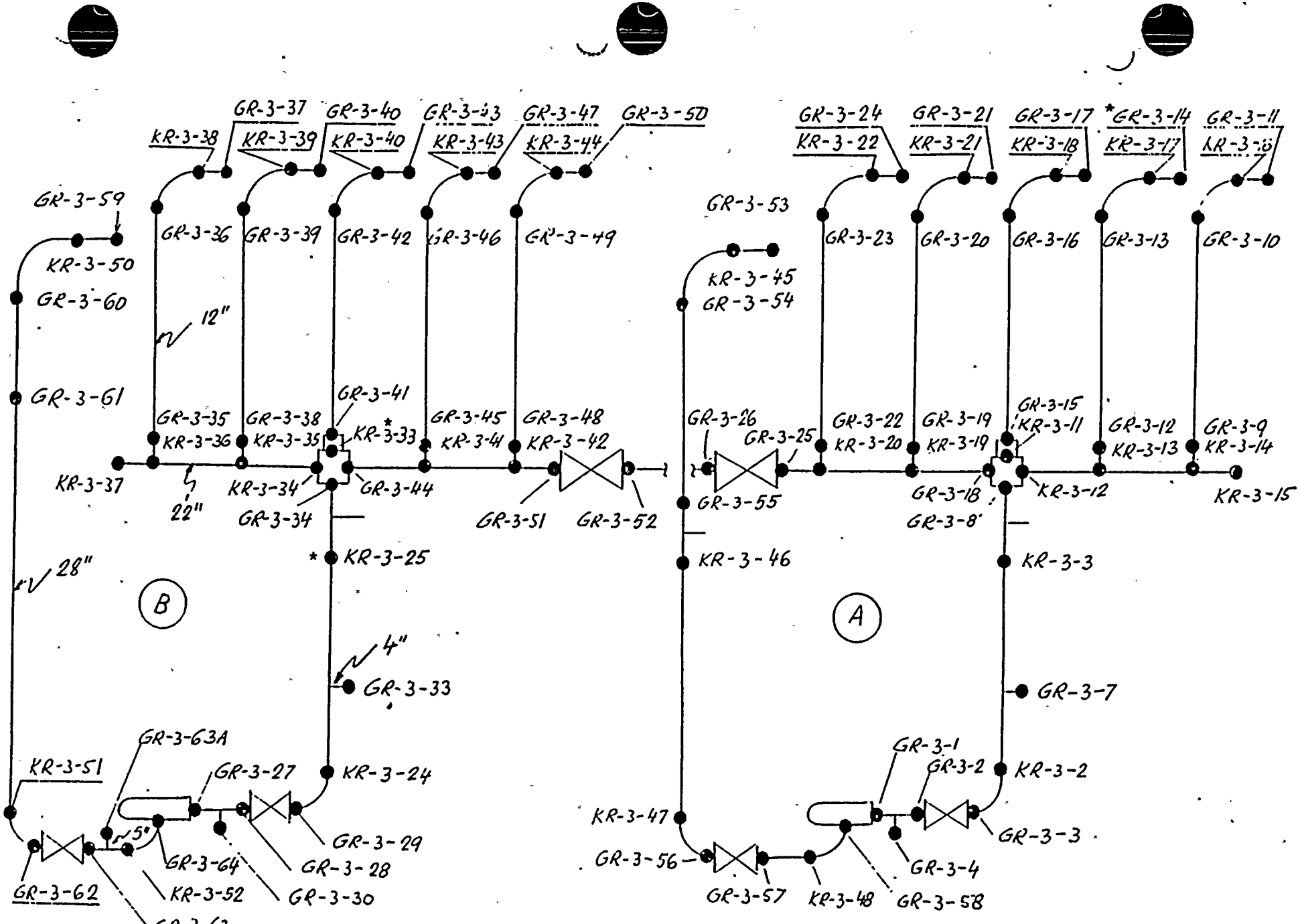


RECIRCULATION LOOP A AND B.

FIGURE 1

* Revised 3/14/84

BFNP -3

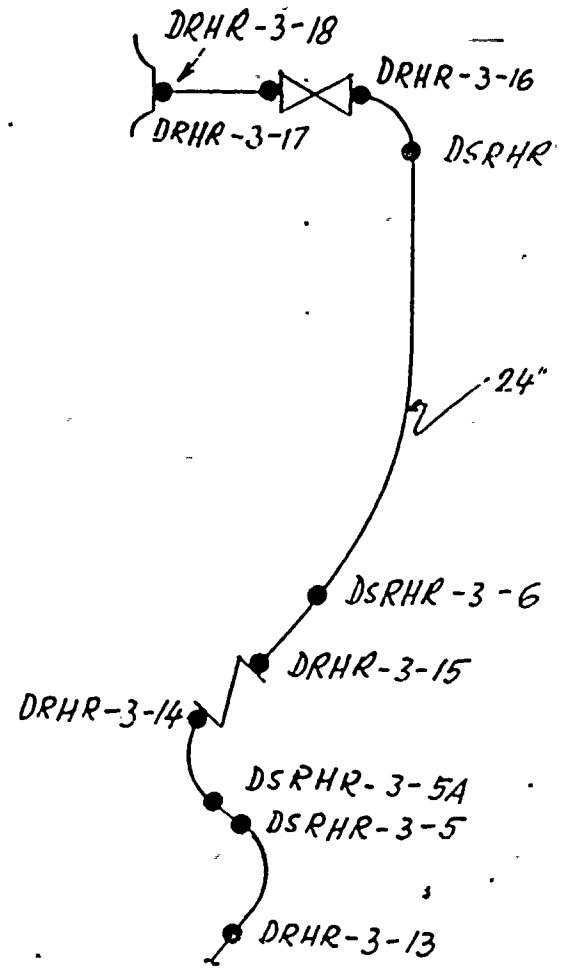


RHR-B LOOP
DISCH.

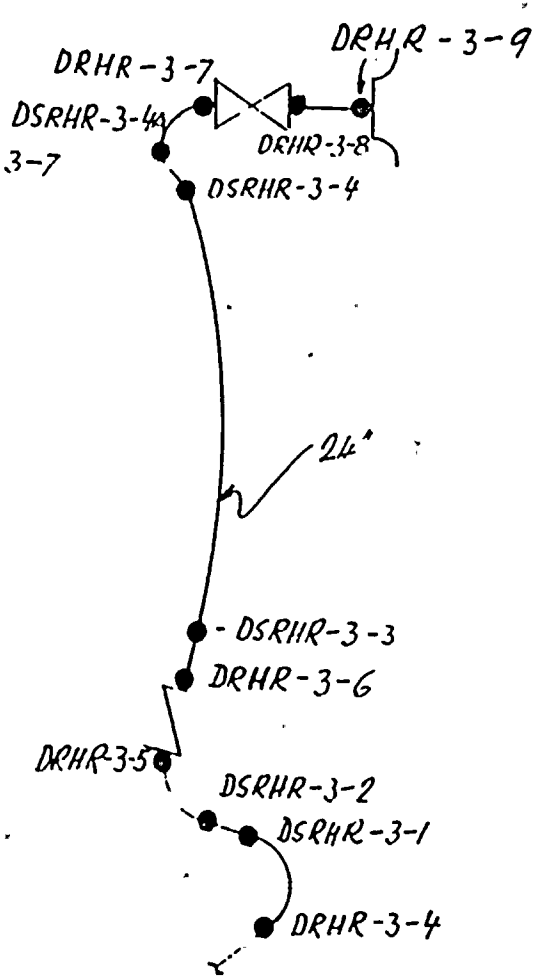


RHR-A LOOP
DISCH

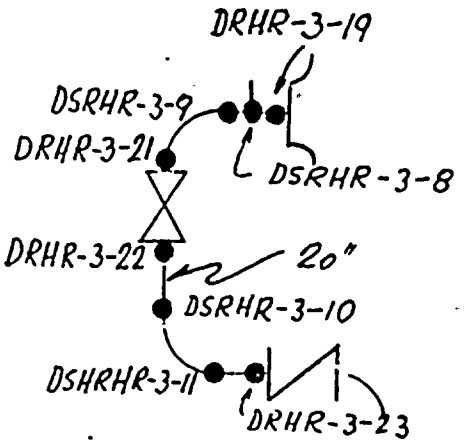


RHR-A LOOP
SUCTION



BFNP-3

FIGURE 2

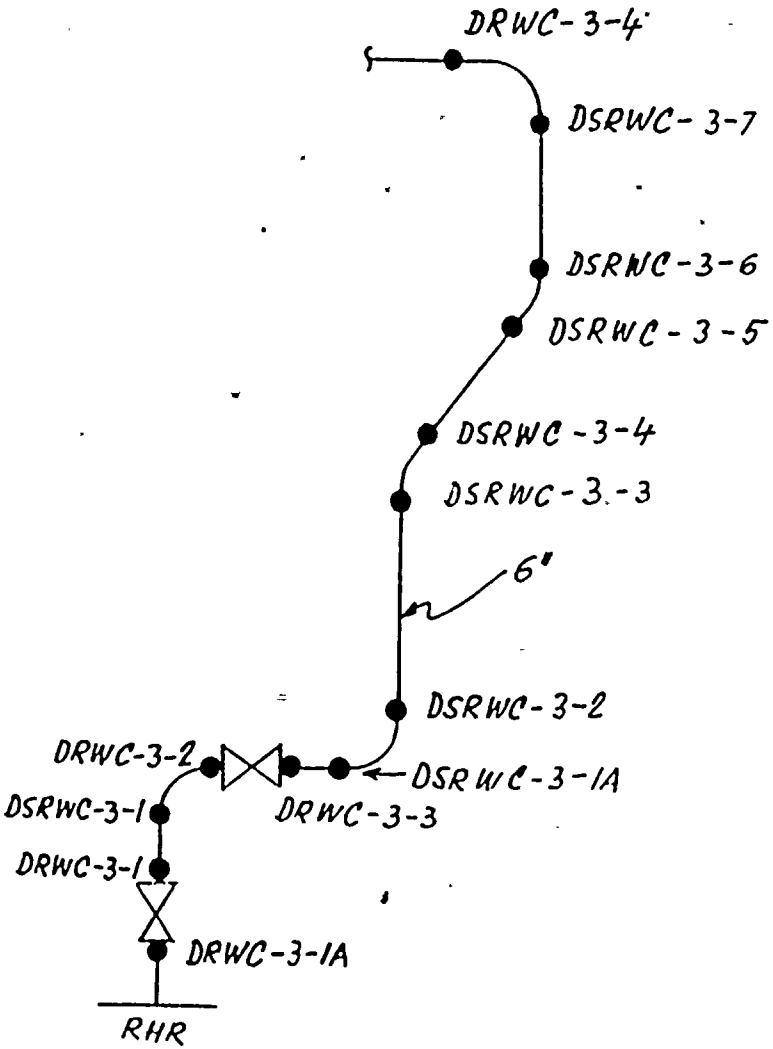


REACTOR WATER CLEAN-UP

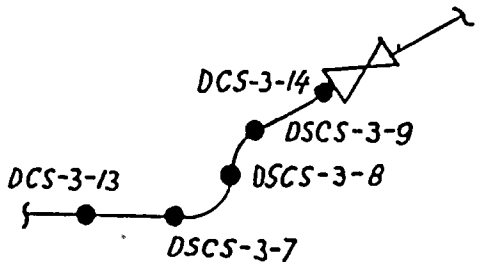


CORE SPRAY - B LOOP

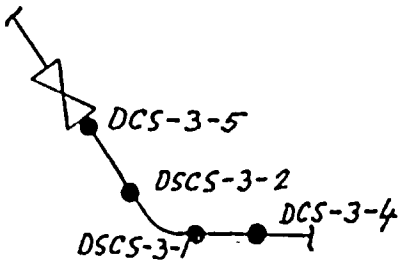


CORE SPRAY - A LOOP



BFNP-3

FIGURE 3

TABLE IA
IGSCC SUSCEPTIBILITY RANKING FOR
BROWNS FERRY 3
RECIRCULATION SYSTEM PIPE WELDS
LOOP A

| Weld No. | SRI | Carbon Content | IGSCC Susceptibility Ranking | Weld Type | Pipe Model Node No. |
|---|---|---|---|---|---|
| GR-3-11 | 1.65 | 0.056 | 1 | Transition To Safe End | 10 |
| KR-3-16 | 1.82 | 0.063 | 1 | Buttweld Elbow | 11 |
| GR-3-10 | 1.75 | 0.063 | 1 | Buttweld Elbow | 13 |
| GR-3-9 | 2.14 | 0.060 | 1 | Buttweld | 14 |
| GR-3-14 | 1.70 | 0.056 | 1 | Transition To Safe End | 20 |
| KR-3-17 | 1.87 | 0.063 | 1 | Buttweld Elbow | 21 |
| GR-3-13 | 1.80 | 0.063 | 1 | Buttweld Elbow | 23 |
| GR-3-12 | 2.21 | 0.060 | 1 | Buttweld | 24 |
| GR-3-17 | 1.84 | 0.056 | 1 | Transition To Safe End | 40 |
| KR-3-18 | 2.10 | 0.063 | 1 | Buttweld Elbow | 41 |
| GR-3-16 | 1.91 | 0.063 | 1 | Buttweld Elbow | 43 |
| KR-3-15 | 2.17 | 0.058 | 1 | Buttweld Reducer | 44 |
| KR-3-11 | 1.42 | 0.060 | 1 | Buttweld Cross | 39 |
| KR-3-12 | 1.63 | 0.060 | 1 | Buttweld Cross | 31 |
| GR-3-18 | 2.00 | 0.060 | 1 | Buttweld Cross | 51 |
| GR-3-8 | 1.68 | 0.060 | 1 | Buttweld T-Cross | 95 |
| GR-3-21 | 1.62 | 0.056 | 1 | Transition To Safe End | 60 |
| KR-3-21 | 1.83 | 0.063 | 1 | Buttweld Elbow | 61 |
| GR-3-20 | 1.81 | 0.063 | 1 | Buttweld Elbow | 63 |
| GR-3-19 | 2.13 | 0.060 | 1 | Buttweld | 64 |
| GR-3-24 | 1.65 | 0.056 | 1 | Transition To Safe End | 80 |
| KR-3-22 | 1.82 | 0.063 | 1 | Buttweld Elbow | 81 |
| GR-3-23 | 1.67 | 0.063 | 1 | Buttweld Elbow | 83 |
| GR-3-22 | 2.03 | 0.060 | 1 | Buttweld | 84 |

TABLE IA
(CONTINUED)
IGSCC SUSCEPTIBILITY RANKING FOR
BROWNS FERRY 3
RECIRCULATION SYSTEM PIPE WELDS
LOOP A

| Weld No. | SRI | Carbon Content | IGSCC Susceptibility Ranking | Weld Type | Pipe Model Node No. |
|---|---|---|---|---|---|
| GR-3-25 | 1.21 | 0.048 | 1 | Buttweld Valve | 257 |
| GR-3-26 | 1.20 | 0.050 | 1 | Buttweld Valve | 256 |
| GR-3-52 | 1.17 | 0.050 | 1 | Buttweld Valve | 253 |
| GR-3-51 | 1.09 | 0.048 | 2 | Buttweld Valve | 252 |
| KR-3-3 | 1.36 | 0.055 | 1 | Buttweld Tee | 117 |
| KR-3-2 | 1.24 | 0.055 | 1 | Buttweld Elbow | 121 |
| GR-3-3 | 1.23 | 0.053 | 1 | Buttweld Valve | 123 |
| GR-3-2 | 1.04 | 0.064 | 2 | Buttweld Valve | 124 |
| GR-3-1 | 1.03 | 0.064 | 2 | Buttweld Pump | 158 |
| GR-3-58 | 1.24 | 0.063 | 1 | Buttweld Pump-Elbow | 157 |
| GR-3-48 | 1.23 | 0.064 | 1 | Buttweld Elbow | 155 |
| GR-3-57 | 1.00 | 0.064 | 2 | Buttweld Valve | 154 |
| GR-3-56 | 1.19 | 0.062 | 1 | Buttweld Valve-Elbow | 153 |
| KR-3-47 | 1.20 | 0.062 | 1 | Buttweld Elbow | 151 |
| KR-3-46 | 1.34 | 0.057 | 1 | Buttweld Tee | 149 |
| GR-3-55 | 1.48 | 0.064 | 1 | Buttweld Tee | 144 |
| GR-3-54 | 1.30 | 0.064 | 1 | Buttweld Elbow | 143 |
| KR-3-45 | 1.60 | 0.064 | 1 | Buttweld Elbow | 141 |
| GR-3-53 | 1.24 | 0.064 | 1 | Transition | 140 |
| KR-3-14 | * | 0.060 | 4 (SHT) | Buttweld | 15 |
| KR-3-13 | * | 0.060 | 4 (SHT) | Buttweld | 19,29 |
| KR-3-19 | * | 0.060 | 4 (SHT) | Buttweld | 59,69 |
| KR-3-20 | * | 0.060 | 4 (SHT) | Buttweld | 78,89,259 |
| KR-3-15 | 1.12 | 0.070 | 1 | Buttweld Cap | 15 |
| KR-3-1 | 1.60 | 0.060 | 1 | Butt Weldolet | 159 |
| KR-3-4 | 1.62 | 0.060 | 1 | Butt Weldolet | 119 |
| KR-3-49 | 1.53 | 0.050 | 1 | Weld Neck Flange | 154 |

*SRI Values Not Calculated For Solution Heat Treated Welds

TABLE IB
IGSCC SUSCEPTIBILITY RANKING FOR
BROWNS FERRY 3
RECIRCULATION SYSTEM PIPE WELDS
LOOP B

| Weld No. | SRI | Carbon Content | IGSCC Susceptibility Ranking | Weld Type | Pipe Model Node No. |
|---|---|---|---|---|---|
| GR-3-37 | 1.56 | 0.056 | 1 | Transition To Safe End | 170 |
| KR-3-38 | 1.72 | 0.063 | 1 | Buttweld Elbow | 171 |
| GR-3-36 | 1.72 | 0.063 | 1 | Buttweld Elbow | 173 |
| GR-3-35 | 2.09 | 0.060 | 1 | Buttweld | 174 |
| GR-3-40 | 1.67 | 0.056 | 1 | Transition to Safe End | 180 |
| KR-3-39 | 1.88 | 0.063 | 1 | Buttweld Elbow | 181 |
| GR-3-39 | 1.81 | 0.063 | 1 | Buttweld Elbow | 183 |
| GR-3-38 | 2.22 | 0.060 | 1 | Buttweld | 184 |
| GR-3-47 | 1.50 | 0.056 | 1 | Transition to Safe End | 220 |
| R-3-43 | 1.65 | 0.063 | 1 | Buttweld Elbow | 221 |
| GR-3-46 | 1.81 | 0.063 | 1 | Buttweld Elbow | 223 |
| GR-3-45 | 2.15 | 0.060 | 1 | Buttweld | 224 |
| GR-3-50 | 1.61 | 0.056 | 1 | Transition To Safe End | 240 |
| KR-3-44 | 1.78 | 0.063 | 1 | Buttweld Elbow | 241 |
| GR-3-49 | 1.70 | 0.063 | 1 | Buttweld Elbow | 243 |
| GR-3-48 | 2.06 | 0.060 | 1 | Buttweld | 244 |
| GR-3-43 | 1.88 | 0.056 | 1 | Transition To Safe End | 200 |
| KR-3-40 | 2.12 | 0.063 | 1 | Buttweld Elbow | 201 |
| GR-3-42 | 1.92 | 0.063 | 1 | Buttweld Elbow | 203 |
| GR-3-41 | 2.17 | 0.058 | 1 | Buttweld Reducer | 204 |
| KR-3-33 | 1.35 | 0.060 | 1 | Buttweld Cross | 199 |

TABLE IB
(CONTINUED)
IGSCC SUSCEPTIBILITY RANKING FOR
BROWNS FERRY 3
RECIRCULATION SYSTEM PIPE WELDS
LOOP B

| Weld No. | SRI | Carbon Content | IGSCC Susceptibility Ranking | Weld Type | Pipe Model Node No. |
|---|---|---|---|---|---|
| GR-3-44 | 1.48 | 0.060 | 1 | Buttweld Cross | 191 |
| KR-3-34 | 1.95 | 0.060 | 1 | Buttweld Cross | 211 |
| GR-3-34 | 1.65 | 0.063 | 1 | Buttweld Tee-Cross | 265 |
| KR-3-25 | 1.31 | 0.064 | 1 | Buttweld Tee | 287 |
| KR-3-24 | 1.20 | 0.064 | 1 | Buttweld Elbow | 291 |
| GR-3-29 | 1.19 | 0.053 | 1 | Buttweld Elbow-Valve | 293 |
| GR-3-28 | 1.02 | 0.055 | 2 | Buttweld Valve | 294 |
| GR-3-27 | 1.01 | 0.055 | 2 | Buttweld Pump | 326 |
| GR-3-64 | 1.22 | 0.063 | 1 | Buttweld Pump-Elbow | 325 |
| KR-3-52 | 1.25 | 0.064 | 1 | Buttweld Elbow | 323 |
| GR-3-63 | 1.01 | 0.064 | 2 | Buttweld Valve | 322 |
| GR-3-62 | 1.01 | 0.062 | 2 | Buttweld Elbow | 321 |
| KR-3-51 | 1.20 | 0.062 | 1 | Buttweld Elbow | 318 |
| GR-3-61 | 0.91 | 0.064 | 3 | Buttweld | 314 |
| GR-3-60 | 1.21 | 0.064 | 1 | Buttweld Elbow | 313 |
| KR-3-50 | 1.32 | 0.064 | 1 | Buttweld Elbow | 311 |
| GR-3-59 | 1.07 | 0.064 | 2 | Transition | 310 |
| KR-3-42 | * | 0.060 | 4 (SHT) | Buttweld | 239,249 |
| KR-3-41 | * | 0.060 | 4 (SHT) | Buttweld | 219,229 |
| KR-3-35 | * | 0.060 | 4 (SHT) | Buttweld | 179,189 |
| KR-3-36 | * | 0.060 | 4 (SHT) | Buttweld | 175 |
| KR-3-37 | 1.12 | 0.070 | 1 | Buttweld Cap | 175 |
| KR-3-26 | 1.60 | 0.060 | 1 | Butt Weldolet | 289 |
| KR-3-23 | 1.58 | 0.060 | 1 | Butt Weldolet | 329 |
| KR-3-53 | 1.54 | 0.050 | 1 | Weld Neck Flange | 322 |
| GR-3-63B | 1.54 | 0.050 | 1 | Weld Neck Flange | 322 |

*SRI Values Not Calculated For Solution Heat Treated Welds

TABLE IC
IGSCC SUSCEPTIBILITY RANKING FOR
BROWNS FERRY 3
RECIRCULATION SYSTEM SAFE ENDS

| | Weld No. (Junction No.)** | SRI | Carbon Content | IGSCC Susceptibility Ranking |
|---|---|---|---|---|
| Inlet Nozzle:* | | | | |
| N2A, N2B | 1 (I) | 1.25 | 0.060 | 1 |
| N2C, N2D | 2 (I) | 1.42 | 0.060 | 1 |
| N2E | 2 (O) | 0.97 | 0.060 | 3 |
| N2F, N2G | 1 (I) | 1.25 | 0.070 | 1 |
| N2H, N2J | 2 (I) | 1.42 | 0.070 | 1 |
| N2K | 2 (O) | 0.97 | 0.070 | 3 |
| Outlet Nozzle: | | | | |
| N1B | 3 (I) | 1.33 | 0.09 | 1 |
| N1A | 3 (I) | 1.33 | 0.08 | 1 |

*See Figures 10 and 11
**I = Inside
O = Outside

TABLE IIA
IGSCC SUSCEPTIBILITY RANKING FOR
BROWNS FERRY 3
RESIDUAL HEAT REMOVAL SYSTEM PIPE WELDS
LOOP A

| Weld No. | SRI | Carbon Content* | IGSCC Susceptibility Ranking | Weld Type | Pipe Model Node No. |
|---|---|---|---|---|---|
| DRHR -3-18 | 1.90 | 0.060 | 1 | Buttweld Tee | 113 |
| DRHR -3-17 | 1.30 | 0.060 | 1 | Buttweld Valve | 111 |
| DRHR -3-16 | 1.51 | 0.060 | 1 | Buttweld Valve | 110 |
| DSRHR -3-7 | 1.51 | 0.060 | 1 | Buttweld | 109 |
| DSRHR -3-6 | 1.04 | 0.060 | 2 | Buttweld | 108 |
| DRHR -3-15 | 1.09 | 0.060 | 2 | Buttweld Valve | 107 |
| DSRHR -3-5A | 1.47 | 0.060 | 1 | Buttweld | 106 |
| DRHR -3-14 | 1.47 | 0.060 | 1 | Elbow | 106 |
| DRHR -3-13 | 1.45 | 0.060 | 1 | Buttweld Elbow | 105 |
| DSRHR -3-5 | 1.45 | 0.060 | 1 | Buttweld Elbow | 105 |
| DRHR -3-19 | 1.74 | 0.060 | 1 | Buttweld | 169 |
| DSRHR -3-8 | 1.84 | 0.060 | 1 | Buttweld | 168 |
| DSRHR -3-9 | 1.90 | 0.060 | 1 | Buttweld | 167 |
| DRHR -3-22 | 1.79 | 0.060 | 1 | Buttweld Valve | 166 |
| DRHR -3-21 | 1.65 | 0.060 | 1 | Buttweld Valve | 165 |
| DSRHR -3-10 | 1.79 | 0.060 | 1 | Buttweld Elbow | 165 |
| DSRHR -3-11 | 1.79 | 0.060 | 1 | Buttweld Elbow | 165 |
| DRHR -3-23 | 1.35 | 0.060 | 1 | Buttweld Elbow | 164 |
| TRHR -3-191 | 1.33 | 0.060 | 1 | Buttweld Elbow | 163 |
| TRHR -3-192 | 1.33 | 0.060 | 1 | Buttweld Elbow | 163 |
| TRHR -3-193 | 1.04 | 0.060 | 2 | Buttweld | 160 |

*Assumed Carbon Value.

TABLE IIB
IGSCC SUSCEPTIBILITY RANKING FOR
BROWNS FERRY 3
RESIDUAL HEAT REMOVAL SYSTEM PIPE WELDS
LOOP B

| Weld No. | SRI | Carbon Content* | IGSCC Susceptibility Ranking | Weld Type | Pipe Model Node No. |
|---|---|---|---|---|---|
| DRHR -3-9 | 1.82 | 0.060 | 1 | Buttweld Tee | 282 |
| DRHR -3-8 | 1.31 | 0.060 | 1 | Buttweld Valve | 280 |
| DRHR -3-7 | 1.56 | 0.060 | 1 | Buttweld Valve | 279 |
| DRHR -3-4A | 1.56 | 0.060 | 1 | Buttweld Elbow | 279 |
| DSRHR -3-4 | 1.61 | 0.060 | 1 | Buttweld Elbow | 278 |
| DSRHR -3-3 | 1.15 | 0.060 | 1 | Buttweld | 277 |
| DRHR -3-6 | 1.27 | 0.060 | 1 | Buttweld | 276 |
| DRHR -3-5 | 1.58 | 0.060 | 1 | Buttweld Valve-Elbow | 275 |
| DSRHR -3-2 | 1.58 | 0.060 | 1 | Buttweld Elbow | 275 |
| DSRHR -3-1 | 1.48 | 0.060 | 1 | Buttweld Elbow | 274 |
| DRHR -3-4 | 1.48 | 0.060 | 1 | Buttweld Elbow | 274 |
| DRHR -3-3B | 0.97 | 0.060 | 2 | Buttweld | 270 |

*Assumed Carbon Value.

TABLE III
IGSCC SUSCEPTIBILITY RANKING FOR
BROWNS FERRY UNIT 3
REACTOR WATER CLEANUP SYSTEM PIPE WELDS

| Weld No. | SRI | Carbon Content* | IGSCC Susceptibility Ranking | Weld Type |
|---|---|---|---|---|
| DRWC-3-1A | 1.12 | 0.060 | 1 | Buttweld Valve |
| DRWC-3-1 | 1.14 | 0.060 | 1 | Buttweld Valve |
| TRWC-3-1 | 1.23 | 0.060 | 1 | Buttweld Elbow |
| TRWC-3-2x1 | 1.24 | 0.060 | 1 | Buttweld Valve |
| TRWC-3-4 | 1.15 | 0.060 | 1 | Buttweld Valve |
| DSRWC-3-1A | 1.22 | 0.060 | 1 | Buttweld Elbow |
| DSRWC-3-2 | 1.21 | 0.060 | 1 | Buttweld Elbow |
| DSRWC-3-3 | 1.20 | 0.060 | 1 | Buttweld Elbow |
| DSRWC-3-4 | 1.18 | 0.060 | 1 | Buttweld Elbow |
| DSRWC-3-5 | 1.30 | 0.060 | 1 | Buttweld Elbow |
| DSRWC-3-6 | 1.32 | 0.060 | 1 | Buttweld Elbow |
| DSRWC-3-7 | 1.30 | 0.060 | 1 | Buttweld Elbow |
| DRWC-3-4 | 1.24 | 0.060 | 1 | Buttweld |
| DRWC-1-4A | 1.61 | 0.060 | 1 | Buttweld |

*Assumed Carbon Value.